MODELING ROLL COMPACTION MECHANICS WITH MULTI-PARTICLE FINITE ELEMENT METHODS

A Thesis

Submitted to the Faculty

of

Drexel University

by

George Robert Weber

in partial fulfillment of the

requirements for the degree

of

Master of Science in Materials Science and Engineering

September 2013

ACKNOWLEDGEMENTS

Above all, I would like to express my tremendous gratitude to my advisor, Dr. Antonios Zavaliangos. It has been an honor for me to have so many great discussions with him over the last four years. I hope that I have absorbed some of his knowledge, wisdom, and ability to find clever simplicity in the most complex of problems. I will always be appreciative of his ever persistent assistance in my academic and personal development.

I would like to thank my committee, Dr. James Rondinelli and Dr. Adam Procopio, for their insights and promotion of my education. Also, special thanks to Sean Garner, Dr. Jerry Klinzing, and Dr. Valantis Tsinginos for their mentorship, as well as the rest of the powder materials research group, alumni included.

Finally, I would like to thank my family and friends for their continued support throughout this process and the Drexel MSE faculty and staff for tolerating all my issues over the years.

TABLE OF CONTENTS

LIST OF TABLES

LIST OF FIGURES

ABSTRACT

Roll compaction is a mechanical processing technique implemented in a wide range of industries including pharmaceutical, food production, chemical, and mining. Due to the large scale and continuous nature of the process, optimization and mechanistic understanding is of great importance. In the past, experimental procedures, continuum models, and finite element methods have been applied in order to analyze the mechanics of roll compaction, and each study has experienced its own set of limitations in regards to its predictive capacity and practical application. The difficulties have primarily included the large number of input parameters and the complex behavior of particle interactions at the local level such as friction, cohesion, segregation, and deformation.

A modern technique, Multi-Particle Finite Element Methods (MPFEM), is employed to offer new insights into the roll compaction process. A two-dimensional model is developed and used to simulate the mechanical response of individual particles during deformation. The effects of parameters such as friction, feed stress, roll speed, density, and velocity fields are observed and investigated at both the macro and particulate levels. Shear banding between the rolls and particle shape behavior are investigated and determined to be crucial factors in roll compaction analysis. The implementation of MPFEM is a new sophisticated tool for evaluating roll compaction and presents significant insight into an important mechanical process.

CHAPTER 1: INTRODUCTION

1.1 Roll Compaction

1.1.1 Overview

Roll compaction is a mechanical processing technique employed in a wide range of industries including pharmaceutical, food production, chemical, mining, and metallurgy [1]. The basic principle of the system is to deposit fine powder between two counter rotating cylinders inducing a compaction of the material into a continuous cohesive briquette.

In most applications, roll compaction is only an intermediate step in the production process. Specific powders are formulated and fed between the rolls for compaction where particulate material becomes agglomerated. The compressed product is then pulverized in a mill and sieved. At this stage, granules, or larger particles composed of agglomerated powder, are extracted from the refined mixture to be used for capsules or tablet compaction. The advantages of granules over the original powder is that granules restrict segregation between the inactive and active ingredients, remain chemically stable, and usually have more controllable flow, compaction, and handling properties for further processing [2].

Because the process does not use liquids to mix and agglomerate powder, roll compaction is classified as a dry granulation process. Dry granulation is beneficial because it avoids many of the common pitfalls of liquid chemical

processing that exist in wet granulation techniques. For example, harmful or eroding chemical reactions, thermal instability, and residual moisture effects are all prevalent issues while granulating in a liquid environment [3]. Dry granulation eliminates these risks by avoiding them entirely.

The mechanics of roll compaction are driven by the boundary conditions of the system; counter rotating rolls draw the material through the compactor by frictional interaction while an oscillatory stress is applied by means of a screw feeder at the entry point. This arrangement ensures that powder continuously transports and compacts between the rolls. During roll compaction, the material behavior becomes very complex. With a high dependence on contact conditions, nonuniform material flow and dynamic variation in hydrostatic and shear internal stresses create many nonlinear characteristics of the powder. This situation produces a number of difficulties when attempting to understand and optimize the process.

To describe a material system with dramatic changes in behavior, the process can be divided into distinct spatial regions where the variation in mechanical mechanisms is not as heterogeneous. In the case of roll compaction, four zones are typically characterized by defining angles along the roll, shown in Figure 1.1.

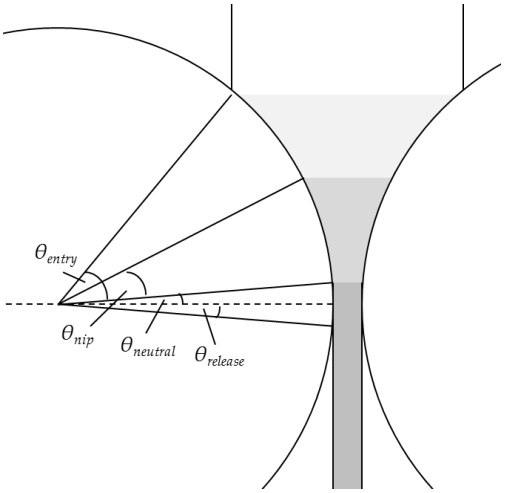

Figure 1.1 Schematic of key angles in the roll compaction system

Above the entry angle, the material is in the feeding zone where it is not yet in contact with the rolls and is directed solely by the feed stress supplied by the screw. As the powder approaches the rolls, the friction between the particle-roll interface promotes motion towards the roll gap. This region is considered the slip zone where particles slip along the roll surface, rearrange, and increase in velocity while the internal stresses remain low. The velocity of the material at the roll surface is lower than that of the roll itself. The powder begins to approach the nip zone, or compaction zone, defined by the nip angle where the particles stick to the roll surface. The velocity of these particles move at the same velocity as the rolls while the pressure develops greatly across the gap width. The increase in stresses creates a region of large densification and irreversible deformation until a maximum in pressure and density is reached. The frictional forces then reverse direction at the neutral angle as the material velocity exceeds that of the adjacent roll surface. The pressure is relieved, and the primary

tribological condition converts back from sticking to slipping in this extrusion zone until the material is finally ejected at the release angle.

In attempt to study and understand this process, empirical and statistical approaches are often undertaken by industry. Although these methods can be effective in optimization and problem solving, they can also be costly, too specific, and undiscerning. Limited information about the macroscale mechanical phenomena is given without intricate and expensive measurement devices while no understanding of local stress states, deformations, and displacements is achieved. Therefore, other techniques must be explored to increase intuition and generalization. Continuum modeling and numerical simulations of the event may be the best methods to introduce the appropriate level of accuracy and localization, offering insight into the varying mechanical mechanisms of roll compaction.

1.2 Mechanical Models

1.2.1 Johanson's Continuum Model

In 1965, J. R. Johanson observed various empirical approaches to roll compaction design and recognized the necessity for a mathematical framework that accounted for the significant number of process parameters [4]. He developed a rolling theory that incorporates an isotropic material governed by friction, cohesion, and compressibility assumptions. In addition, the powder is restricted to the inherent geometric boundary conditions and the Jenike-Shield

effective yield function which provides a flow criterion during plastic shear deformation [5].

The plain strain model separates the underlying mechanics into two specific regions of material behavior corresponding to the positional dependent wall-particle frictional interaction. In the first area, above the nip angle, the particles are permitted to slip along the roll surface. This constraint, in conjunction with information about the feed pressure, allows for computing the pressure distribution from the Jenike-Shield flow criterion. The required input parameters for the friction system include the effective angle of friction and the surface friction angle, which can both be experimentally measured.

The region below the nip angle is analyzed by assuming that no slip occurs between the roll surface and the contacting powder. This condition ensures that all material in the nip region is continuously densified until exiting at the roll gap. The pressure distribution is then determined by employing a conventional pressure-density relationship for powder compaction,

$$\frac{\sigma_a}{\sigma_b} = \left(\frac{\gamma_a}{\gamma_b}\right)^K \tag{1.1}$$

where σ_a and σ_b are applied pressures, γ_a and γ_b are mass densities corresponding to each respective pressure, and K is the material compressibility constant. Following this experimental law and the continuity of mass, the pressure at any angle θ along the roll in the nip region is given by

$$\sigma_\theta = \sigma_\alpha \left[\frac{\left(1 + \frac{S}{D} - cos\alpha\right) cos\alpha}{\left(1 + \frac{S}{D} - cos\theta\right) cos\theta} \right]^K \tag{1.2}$$

where α is the nip angle, σ_α is the pressure at the nip angle, S is the roll gap width, and D is the roll diameter.

One of the most notable benefits of Johanson's model is its ability to theoretically predict the nip angle of a particular material undergoing roll compaction. This result has been experimentally validated and found to be generally accurate with some dependence on roll gap width [6]. Johanson reasoned that the nip angle could be computed by equating the pressure gradient of the slip region with that of the nip region. This argument is similar to energy minimization. The derivative of the pressure with respect to the rolling direction is approximated above the nip angle and calculated below to yield two equations equivalent at the intersecting point. This concept is best observed through graphical representation, Figure 1.2.

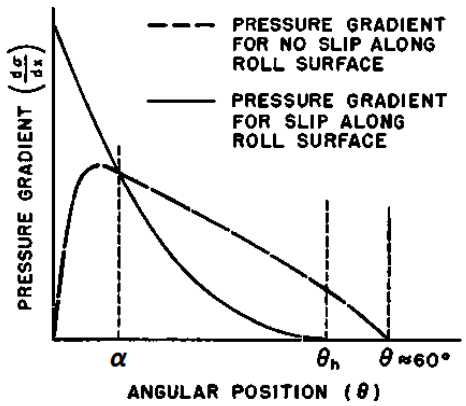

Figure 1.2 Vertical pressure gradient versus angular position in roll bite [4]

With the nip angle and pressure distribution of each region known, Johanson continued the analysis by studying variation in process parameters. The pressure distribution along the roll was integrated, yielding total roll force and total roll torque, to provide a list of output variables that were more relevant to the practical application of the model. Some of the parametric studies performed include observing the effects of compressibility, internal friction angle, wall friction angle, and the ratio of roll gap width to roll diameter on outputs such as nip angle, roll force, roll torque, and maximum pressure. A comprehensive discussion of each of Johanson's parametric investigations can be attained in his original paper [4], but a general conclusion is that each material property has a significant influence on the necessary mechanical operating conditions of roll compaction. In addition, the nip angle was affected by friction and compressibility, but remained relatively unchanged with geometric deviations such as increasing roll gap width and roll surface indentation depth. The work emphasizes the importance of understanding material behavior when considering experimental or commercial design, and it demonstrates an explanation why some powders densify in a specific system state while others cannot.

1.2.2 Slab Method

Another important model that was first developed in 1966 by Katashinskii [7] has been referred to as the "slab method" in the literature. Upon creation, it was primarily designed for application in rolling metal powders and

has since been adapted to other various material systems including pharmaceutical powders. The primary advantage of the slab method over Johanson's rolling theory is the improved material description, allowing more complex yield criteria to be implemented.

The analysis process includes examining the equilibrium of an infinitesimal slab of material moving through the roll compactor, applying a constitutive plasticity model, and solving the resultant differential equation with appropriate boundary conditions. Similar to Johanson's model, the slab method introduces the powder as a continuum under plain strain conditions and assumes that dynamic and gravitational body forces are negligible. The forces acting on the infinitesimal element are projected onto the direction of rolling in order to formulate a one-dimensional equilibrium equation. Katashinskii writes this force balance as

$$h_x d\sigma_x + \sigma_x dh_x - P_x dh_x + t_x \frac{dh_x}{tan\alpha_x} = 0 \qquad (1.3)$$

where the σ_x is the mean stress in the x direction (rolling direction), h_x is the distance between rolls, P_x is the pressure, t_x is the shear force due to contact friction, and α is the angle along the roll. Katashinskii uses Eq. (1.4) to determine the pressure distribution in the slip and nip zones, referred to as the "lag zone" in his paper, and for the extrusion zone, or "forward slip zone", he assumes a simplified form of the same equation,

$$h_s d\sigma_x - 2\mu R P_x d\alpha_x = 0 \qquad (1.4)$$

where μ is the coefficient of friction, R is the radius of the roll, and α_x is the angle along the roll. A plasticity criterion is introduced,

$$\sigma_1 - \sigma_3 = K_Y \tag{1.5}$$

where σ_1 is the maximum principal stress, σ_3 is the minimum principal stress, and K_Y is a yield stress, to create a relationship between $d\sigma_x$ and dP_x and can be viewed as the major difference between Katashinskii's original work and later slab method models. Following Katashinskii, the metal powder begins plastic deformation at the contact zones where the difference between the maximum and minimum principal stresses exceeds an induced yield stress K_x. In addition, this yield strength value is assumed to increase linearly as the material is drawn through the rolls in the slip and nip areas so that

$$K_x = K\left(1 - \frac{h_x - h_s}{\Delta h}\right) \tag{1.6}$$

where K is the final value of the yield strength, h_s is the final thickness of the strip, and Δh is the total change in thickness. The final yield strength is reached at the neutral angle and is then held constant through the extrusion zone. Combining the whole analysis and solving the differential equations, Eq. (1.3) and Eq. (1.4), Katashinskii provides analytical expressions for the pressure distributions above and below the neutral angle and compares the results to past experiments. The model prediction and experimental data are depicted in Figure 1.3 for iron powder and correlate closely.

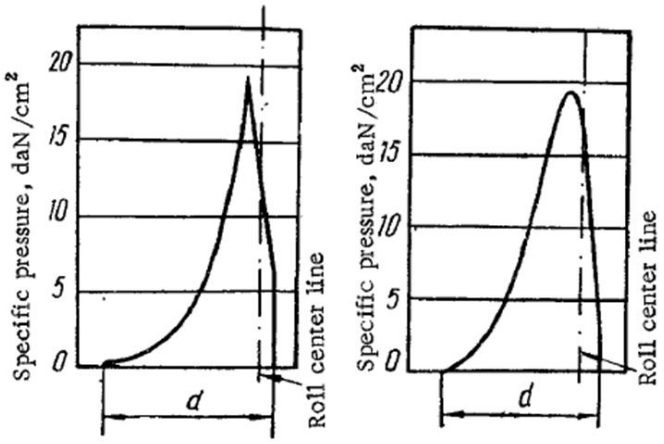

Figure 1.3 Pressure distribution of iron powder along roll from (A) Katashinskii's model and (B) experimental data [7]

Since the first presentation of the slab method, efforts were conducted to advance the procedure into more complex material systems. Specifically, the pharmaceutical industry maintains interest in the roll compaction of powders, and researchers have implemented plasticity laws suitable for this application. The Kuhn-Downey yield criterion was proposed for roll compaction by Dec [8], and later, a porous plasticity model by Cunningham in Chapter 5 of [9].

Dec's approach consisted of separating the evaluation of frictional shear stress into a piecewise function dependent on the point at which the yield criterion is exceeded. Initially, the frictional stress is dependent on the coefficient of friction and pressure but evolves into the yield function once a limit is surpassed. In addition, the coefficient of friction and Poisson's ratio are treated as functions of density throughout the analysis and are both experimentally determined. With this methodology, a calibrated model was achieved for lignite

and sodium chloride and generally agreed with equivalent experiments (see Figure 1.4).

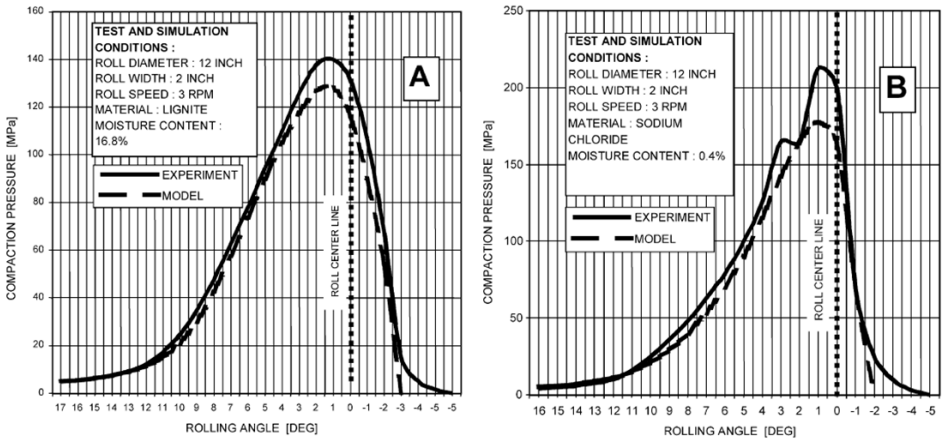

Figure 1.4 Comparison between computed and recorded pressure distribution in roll nip during compaction process [8]

Cunningham also implements a slab analysis to perform parametric studies on the effects of input variation on the behavior of microcrystalline cellulose, a common pharmaceutical excipient, in roll compaction. A yield function of symmetric elliptical form dependent on pressure is utilized to characterize material behavior. The modeling process begins similar to Katashinskii and Dec's examinations with the equilibrium equation for an infinitesimal element of material. The angular form is given by

$$hd\sigma_x + R(p_r sina \pm t_r cosa)da = 0 \qquad (1.7)$$

where a is the angle along the roll and the plus and minus signs correspond to whether the slab is above or below the neutral angle, respectively. At this point, functional forms of the relative density's dependence on roll angle are postulated

for the slip and nip regions dependent on parameters such as volumetric strain, initial relative density, nip angle, and entry angle. The porous plasticity model is then applied. The material behavior is restricted to the yield function, F, expressed by

$$F = A(RD)q^2 + B(RD)p^2 - 1 = 0 \quad (1.8)$$

where A and B are coefficients dependent on relative density, q is the equivalent stress, and p is the hydrostatic pressure. Then, a plastic flow rule and Coulomb friction law are applied. Cunningham provides two new features in the slab model that are not found in Katashinskii or Dec's work which entail removing the implicit incompressibility assumption for stress in the roll depth direction as well as offering an analysis of elastic unloading after the strip moves through the roll gap. The resultant differential equations of the analysis were solved numerically for the properties of microcrystalline cellulose, and parametric studies were executed to observe the effects of processing inputs such as entry angle, coefficient of friction, relative density, feed stress, material properties, and geometry. A plot of the pressure distribution along the roll is given in Figure 1.5.

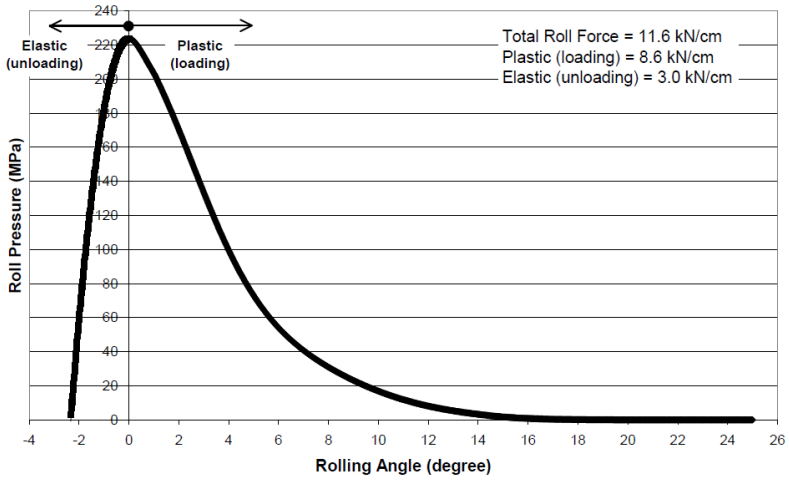

Figure 1.5 Pressure profile including elastic unloading [9]

The slab method allows great benefits in affording analytical or resource efficient solutions to a complex problem. With a calibrated model, the consequence of variations in process parameters can be relatively quickly assessed, and the plasticity functions can also be adapted to different systems capturing specific material behavior. However, some slab analyses require calibration variables that are difficult to fully measure and define experimentally. Two and three dimensional effects and boundary conditions are also not sufficiently accounted for and may greatly influence material behavior; for example, the rotation of the screw feed and powder particle flow. Despite the challenges and shortcomings, the continuum models offer excellent insight into the complexity of this multi-parametric system.

1.2.3 *The Modified Drucker-Prager Cap Model*

In an attempt to gain further insight into the mechanical behavior of powder materials during compaction, other plasticity models have been adopted

and determined to be experimentally validated. Particularly, the Drucker-Prager Cap (DPC) model has proven to accurately describe various qualities of particulate materials that others cannot. The DPC model was originally developed by Drucker in 1957 as a theory for plastic deformation of soils [10] but has been updated and modified for other applications over the last 50 years. Sandler and DiMaggio [11, 12] significantly adapted it to geological applications in the 1970's while Weber and Brown [13] modified it further for use in the study of metal powders during the 1980's and 1990's. Finally, a modified density dependent version has been formulated for pharmaceutical powders and developed to be used in engineering applications [8, 9, 14-16].

The modified DPC model proposes a continuous, compressible, and isotropic material constrained to a distinct yield surface in hydrostatic pressure – Mises equivalent stress space. The yield surface can be divided into two major individual boundary regions, Figure 1.6. The first of these boundaries is the shear failure line which promotes shear flow as the material plastically deforms at low pressure.

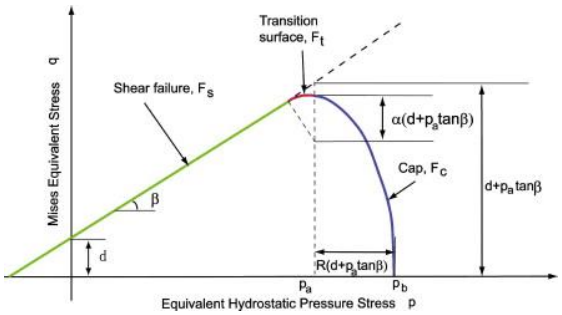

Figure 1.6 Drucker-Prager Cap model yield surface in the *p* - *q* plane [14]

This portion of the surface is most simply defined as a linear function in equivalent stress (q) - hydrostatic pressure (p) space and is given by

$$F_S(q,p) = q - d - ptan(\beta) = 0 \tag{1.9}$$

where d is considered to represent cohesion and β is the internal angle of friction. As the shear failure line begins to be exceeded, the material behavior transitions from elastic deformation to irrecoverable shearing. On the other hand, as the stress state approaches the "cap" surface at higher pressures, different particulate phenomena control the plastic flow. The cap is a density dependent yield surface that hardens the material as plastic deformation continues. It is uniquely defined for a constant relative density and will translate and scale in stress space as this parameter is varied. The surface is expressed by

$$F_c(q,p) = \sqrt{(p-p_a)^2 + \left[\frac{Rq}{1+\alpha-\frac{\alpha}{cos\beta}}\right]^2} - R(d + p_a tan\beta) = 0 \tag{1.10}$$

where p_a and R are material parameters determining the plastic strain and curvature of the cap, and α is a term used to connect the shear failure line and the cap surface. This α value defines a third region on the yield surface which ensures a smooth transition for numerical purposes. The full three dimensional yield surface is shown in Figure 1.7 and illustrates the two major boundaries as well as the transition zone for increasing relative densities.

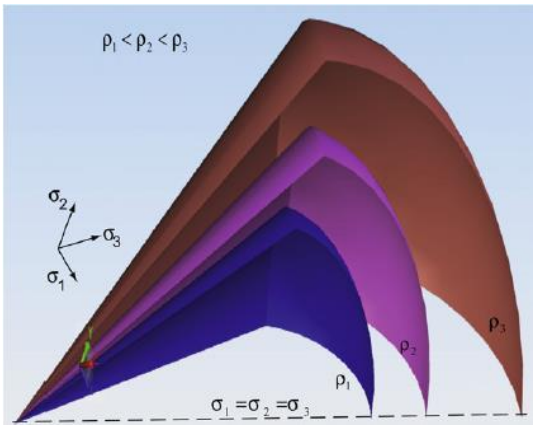

Figure 1.7 Schematic of a density-dependent Drucker-Prager Cap model for 3D yield surfaces in principal stress space (1/4 model) [14]

Finally, a non-associated and associated flow rule is applied to the shearing and cap regions, respectively, to describe the plastic strain upon yielding. The DPC model's overall description of plastic behavior summarizes the major macroscopic qualities of powder materials during compaction. However, the unloading process is primarily an elastic, nonlinear event that must be treated separately. The bulk modulus and shear modulus are computed from the unloading curves as functions of hydrostatic pressure and equivalent stress. In other implementations of the DPC model, these terms have been held constant and may have affected the resulting accuracy upon unloading.

The practical advantage of developing the DPC model for porous materials is that it can be relatively easily calibrated for application in compaction processes. Six major parameters (β, d, p_a, p_b, R, α) must be quantified to fully characterize the yield surface and two elastic parameters, K and G, are acquired to define the elastic unloading mechanics. With fairly standard

compaction laboratory equipment, a reasonable number of experiments can be executed to completely describe the system. Simple tension, pure shear, diametrical compression, and simple compression are all common tests that have unique paths in *p*-*q* space and eventually reach the shear failure line at different points (Figure 1.8) along the curve.

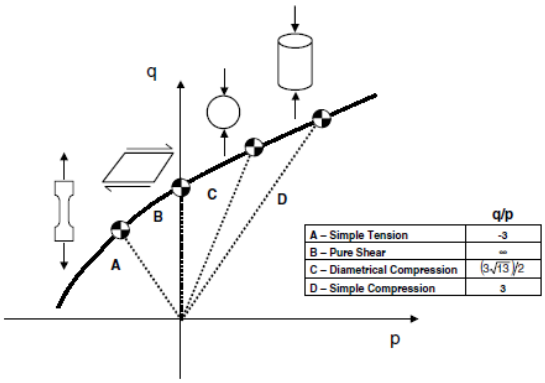

Figure 1.8 Schematic representation of a failure locus near the shear stress [17]

Only two of these experiments are required to plot the linear boundary of the yield surface and thus calculate the cohesion and internal friction angle values. The cap parameters are measured by devising a loading path that will contact the cap curve at failure, and this yielding point is used to evaluate R and p_a. With these factors known, p_b is determined from

$$p_b = p_a(1 + Rtan\beta) + Rd \tag{1.11}$$

and α is termed a small number between 0.01 and 0.05. Lastly, K and G are computed from a stress-strain unloading curve. The experiments can then be repeated for numerous values of relative density in order to supply a family of

yield surfaces showing the full dependency on density. For further reference on the calibration process, the entirety of the methodology is meticulously explained in [14].

The DPC model retains its generality throughout the derivation and, therefore, can be utilized to understand the mechanics in most compaction procedures. This fact allows the material description to not only apply to simple die compaction but also problems with more complex boundary conditions such as roll compaction. In addition, the model addresses the behavior in three dimensional space, permitting the opportunity to recreate a complete, realistic system.

1.2.4 Finite Element Method

With the macroscopic accuracy of the DPC model for porous materials, it is of importance to apply the technique to numerous systems and observe the outcomes. However, due to the abundance of conditions and relationships, numerical computation appears to be the best solution for calculating the output parameters.

The finite element method (FEM) is a numerical technique for approximating the mechanics of a system. A material geometry is mapped into a finite number of nodes and elements, and each element is assigned a volume, constitutive material behavior, and specific set of boundary conditions. The nodal displacements are approximated to a certain degree dependent on the chosen interpolation function, and the deformed state is analyzed. FEM has

grown rapidly over the last decades as computational software and visual packages have become simpler and more powerful to use. The controllable degree of accuracy and ability to handle complex geometries and boundary conditions also led to the commercial adaptation of FEM. It has introduced many solutions to modern problems that could not have been discovered in other ways.

Because of the excellent advantages of FEM solvers, they have been applied to the area of powder compaction as well as many other fields. The procedure allows the usage of the DPC model to assist in the understanding of die and roll compaction. The difficulties in analytically managing the many processes that are governed by the yield surface are not present when solved numerically. For example, continuity issues may arise while attempting to use piecewise functions for evaluating plastic flow type criteria whereas a computer program can maneuver through this dilemma using simple logic statements.

For die compaction, the flat and curved faced die simulations shown in Figure 1.9 were observed through FEM analysis and produced accurate results.

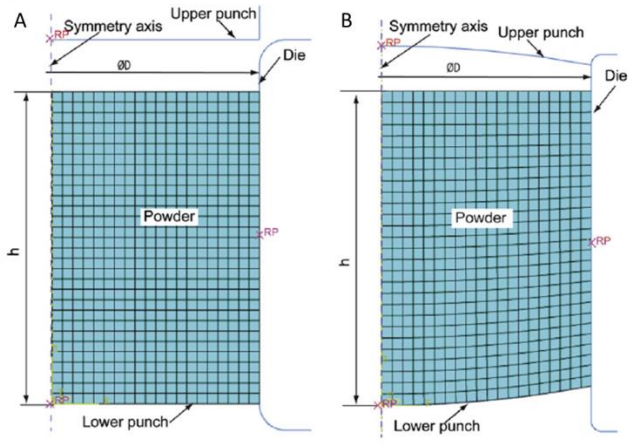

Figure 1.9 Finite element model of die compaction using (A) flat-face punches and (B) concave face punches [14]

The FEM analysis was capable of predicting the unloading portion of the force – displacement plot, and it could capture features of the pre- and post-ejection tablet such as nonuniform density distributions and regions of high stress. In addition, a curved geometry was compared and found to match common failure forensics observations for pharmaceutical tablets.

Another success of the DPC model combined with FEM is the ongoing analyses of roll compaction. This task was undergone several times in the last decade [2, 8, 9, 18, 19] and has emphasized the vast number of influential process variables as well as their significant effects on the system. Dec et al. formulated an FEM approach to roll compaction and showed not only the pressure distribution along the roll but also the shear stress distribution [8]. In addition, the effects of friction and feed stress were tested in order to observe their influence on the stress distributions, and a velocity plot in the rolling direction was generated from the data. These results provide new insights into the

material mechanical behavior and flow and yield methods for predicting the nip and neutral angles of the system.

An extension of this work was performed by Cunningham [2, 9] to assist in the understanding of process parameter variations for roll compaction design. A two dimensional and three dimensional model were based on the modified DPC criteria and simulated for numerous values and functions for roll friction, entry angle, feed stress, geometry, side seal friction, and inlet velocity. An illustration of the FEM mesh, geometry, and analysis features is displayed in Figure 1.10.

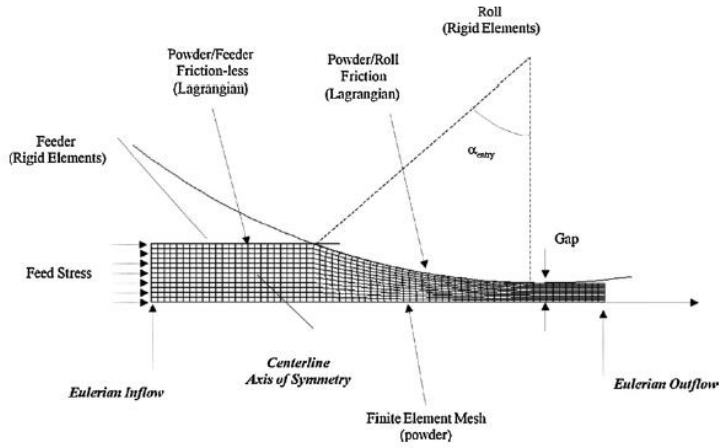

Figure 1.10 Schematic of finite element mesh for roller compaction with corresponding notation [2]

Cunningham's work is executed with the explicit integration procedure in Abaqus and utilizes adaptive meshing, mass scaling, and symmetry across the rolling direction. Assumptions include plane strain conditions, negligible gravitational and inertial effects, rigid rolls, constant feed stress, and Coulomb

friction. The model is implemented for combinations of input parameters and stress distributions, maximum pressure and relative density, and velocities are observed. Similar to other models of roll compaction, the pressure profile is computed along the roll and shown here in Figure 1.11.

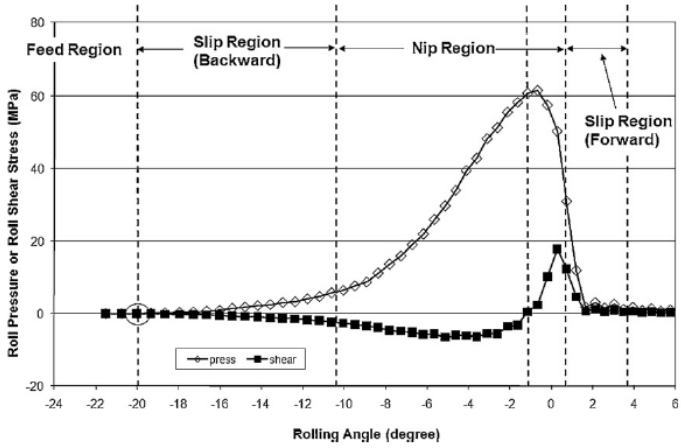

Figure 1.11 The roll pressure and roll shear stress versus rolling angle for example simulation [2]

The maximum pressure occurs at the point of zero shear stress, or the neutral angle, which lays a few degrees above the centerline of the rolls. Also, it is interesting to note that the shear stress reaches a maximum three times larger after the neutral angle compared to that of before it.

Parametric studies are performed beginning with an analysis of powder/wall friction. The coefficient of friction is tested as different functions of pressure, and the maximum relative density and maximum pressure are recorded. The trend reveals a declining maximum density as wall friction is decreased. Likewise, decreasing the entry angle has the same effect. With a

larger entry angle, the powder has a larger range of distance to undergo the densification process. The feed stress also has a crucial relationship with the entry angle. This initial stress mainly acts to predensify the material in the slip region before entrance into the compaction zones. Therefore, a higher feed stress will result in a larger maximum pressure between the rolls. Moreover, a large feed stress will require a greater entry angle to achieve the same maximum density due to the increased area of contact.

The constant feed stress is often not maintained in a commercial roller compactor due to the oscillatory motion of the screw feed system [20]. Therefore, Cunningham employed a three dimensional model with a sinusoidal loading to help understand the effects of the screw feed. It was determined from the simulation that this loading function induces a fluctuating density distribution within the briquette similar to that seen in experiments. The maximum roll pressure is forced to the center of the strip and decreases as the side seal is approached. This significant variation is not observed under constant feed stress. Another prominent three dimensional effect is the friction due to the side seal. The friction along this boundary does not have a dramatic impact but is shown to slightly decrease the pressure and density near the edge of the rolled material. With the combination of the oscillatory feed stress and side seal friction, a substantial amount of nonuniformity is introduced across the thickness of the briquette.

The FEM model serves to offer new insights into the roll compaction process that may be very difficult to describe through continuum mechanics. The DPC yield surface has proven to be sufficiently accurate in predicting die compaction behavior so it is of great benefit that FEM allows its application in roll compaction as well. On the other hand, numerous features of powder behavior may never be fully captured by the DPC model. The calibration methods rely on experiments that cannot inherently capture behavior below a certain minimum relative density. This value is determined by the minimum relative density required to form a solid specimen for testing, which is a major disadvantage relative to discrete modeling methods. Thus, the determination of behavior is dependent on tableting properties rather than the overall powder material characteristics. Furthermore, there are many phenomena occurring at the particulate scale that are impractical to include in a macroscopic model such as particle shape, particle size distribution, multicomponent mixing and segregation, shear banding, defects, stress networks, and effects of coordination number. Complete confidence in the definition, calculation, and calibration of DPC input may be questioned for parameters such as friction, cohesion, unloading variables, and plastic flow behavior. Therefore, the representative volume of the system may be too large to completely describe the mechanical performance.

1.2.5 The Discrete Element Method

As a pioneering effort to acquire understanding of the particulate behavior of soils, powders, and other porous materials, the discrete element method (DEM) was formulated. In its simplest form, DEM proposes modeling granular media as a finite number of discrete spheres and assumes a spring-like interaction between each contact. This technique was first introduced for granular media in the 1970's [21] and has since expanded in many fashions. With advances in computational resources and parallel computing, simulations have exceeded well over one million particles in three dimensional analyses. This growing number of individual spheres provides increasingly accurate approximations to realistic multibody systems.

The major developments in DEM for granular compaction and flow rely heavily on the contact laws, frictional assumptions, and allowable degrees of freedom. Observable macroscopic phenomena in porous media, such as plasticity, can be captured by the contact interaction relationships between particles, and the assumed yield surfaces in continuum mechanics can be probed by investigating various triaxiality states of granular assemblies [22]. DEM allows for studying standard powder characterization tests such as compression, tension, shearing, and other configurations. Not only are stress strain curves generated from these analyses, but also micromechanical responses relating to local density and coordination number are computed.

The ability to manage large quantities of particles for modeling granular systems renders DEM an appealing technique. However, with this benefit, local particle mechanics must be significantly simplified. The contact interaction laws are thus responsible for describing the deformation, friction, elasticity, plasticity, rotation, and other types of behavior, and a single function often struggles to handle each aspect or becomes impractically complicated and specific. A persistent challenge for DEM has been accurately predicting experimental quantities at high densities. This condition is highly dependent on updated volume and contact area information which are not naturally handled by the basic DEM principles. Although current research is addressing this problem and approving upon a solution with new techniques [23], the full behavior of particles at high density remains a complicated issue for DEM. In addition, other factors that are not easily described by contact interactions include particle rolling, loading history, deformation history, volume dependent properties, and coupling between multiple instances of these concerns.

1.2.6 The Multi-Particle Finite Element Method

Because of the great benefits of FEM in accurately solving highly nonlinear elasto-plastic problems and the advantages of DEM in recording the discrete nature of granular media, a new method was proposed, termed Multi-Particle Finite Element Method (MPFEM), to combine the strengths of each procedure. The mechanical system is discretized into individual deformable particles and solved with the finite element procedure. In the mid 1990's and

early 2000's, a few initial examples of MPFEM began to appear in the literature [24-28] but were applied to dynamic shock problems or resembled unit cell methods for compaction with a low particle count. A full presentation and validation of the methodology was comprehensively studied by Procopio and Zavaliangos [29, 30] based on an earlier introduction to the work [31]. This research is the foundation for the current work and will be briefly discussed.

Unlike many DEM simulations, MPFEM is primarily restricted to two dimensional analyses due to demand for computational resources. Therefore, particles are modeled as deformable circles and meshed with quadrilateral continuum elements. The selection of the mesh is judiciously chosen to maximize solution accuracy while minimizing CPU time. The optimized mesh biases each particle surface with 72 of the 132 total elements per particle and is illustrated in Figure 1.12.

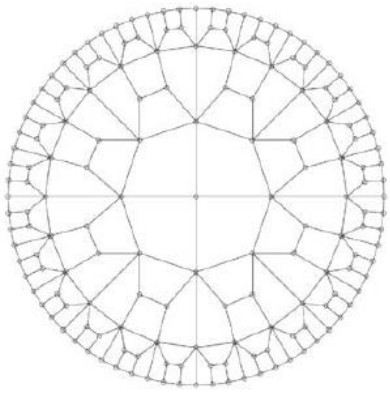

Figure 1.12 Mesh used in MPFEM work [29]

The mesh is then evaluated in various packing configurations and compared against a very fine mesh comprised of 2700 elements. The results of this study, shown in Figure 1.13, validate the application of the customized mesh.

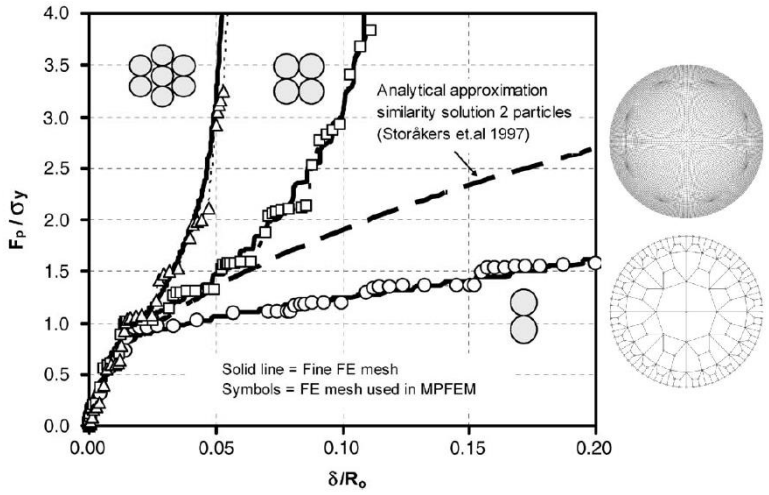

Figure 1.13 Normalized interparticle force (c) as a function of interparticle strain for a simplified 1/4 cylinder under normal, simple cubic, and hexagonal loading [29]

The MPFEM model is executed using the explicit integration procedure in Abaqus, a commercial FEM software. The explicit procedure is very important in the modeling of this problem because of its high nonlinearities and contact dynamics. An implicit solver would not be capable of convergence on such a system. The initial configuration of the particles is a random packing created by loosely placing particles inside the boundary region and densifying them through applying inward velocities. A convergence study was performed to test the number of particles necessary to relieve the effects of the rigid walls, and it was determined an 800 particle system was sufficient considering simulation

time restraints. A particular stress state is created for the material by moving the rigid wall boundaries at predefined velocities. This motion allows different triaxialities to be imposed on the particles. Also, the MPFEM takes advantage of mass scaling and a priori defined contact pairs within an optimized range. Both of these techniques dramatically lower total simulation time and do not significantly affect output if implemented correctly. The particle to wall friction is held at zero for all tests, and the particle to particle friction is varied. For cohesion, the two extreme limits, no cohesion and perfect cohesion, are studied due to FEM software constraints.

With the model parameters outlined, many simulations were performed to compare the method against other models, understand the evolution of coordination number, determine macroscopic stresses, and observe particle rearrangement, nonaffine motion, and rotation. In addition, various triaxiality states were generated in order to probe the yield surface of the aggregate material. Each of these results displays the usefulness of MPFEM and its potential in studying the compaction process. Other methods cannot fully account for some of these features, especially at high densities, so MPFEM offers great insight into the behavior of particulate material.

CHAPTER 2: MODELING APPROACH AND TECHNIQUES

2.1 Objectives

2.1.1 Roll Compaction Model Generation

With past knowledge of MPFEM techniques available, the present work aims to apply this methodology to the roll compaction process. In order to draw conclusions about an upscaled system, the model must be independent of initial configuration, properly mass scaled, reach steady state, and retain enough particles to remain representative. These qualities ensure that results are meaningful and reflective of the mechanical process. A validated model will promote observing phenomena in roll compaction that are typically too difficult to investigate with continuum mechanics or DEM approaches. Thus, MPFEM can offer new insights into the complex process. This work acts to explore some of the advantages of multi particle analysis for roll compaction and lay a foundation for future work in the area.

2.1.2 Parametric Studies

After demonstrating an established model, a presentation of the effects of variation in input parameters will be provided. Some process parameters include friction, roll velocity, and feed stress. In addition, comparisons to uniaxial die compaction and systems of differing particle shape will be demonstrated. Outputs such as total roll force, total roll moment, velocity fields, pressure distributions, nip and neutral angle approximations, and equivalent

plastic strain will be used in the study to characterize the mechanical behavior of the granular media. Finally, shear banding and roll compaction steady state will be discussed in detail. MPFEM has many tools to offer and is an excellent technique for understanding powder processes. A goal is to present the data in order to influence future experiments and questioning into the underlying mechanisms of roll compaction micromechanics.

2.2 Particle Mesh and Packing

2.2.1 Particle Mesh

Because of computational intensiveness, the MPFEM model for roll compaction is restricted to a two dimensional analysis, and, therefore, the primary particle shape is chosen to be circular. However, other 2D shapes were examined as well. FEM analysis requires that the material of the system must be meshed with nodes and elements. The nodal displacements are determined by the finite element solver and are used to approximate the stresses and strains for the entire model. Given that the majority of mechanical interaction and deformation exists at the surface of each particle, it is important that the nodes are biased to this end. The optimized mesh implemented in Procopio's work [29] is determined to be sufficient for the roll compaction analysis as well and is recreated here in Figure 2.1.

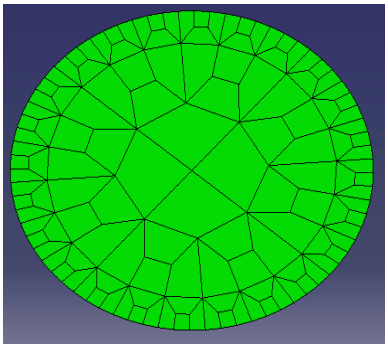

Figure 2.1 MPFEM mesh for circular particles

The mesh includes 169 nodes and 132 elements at which 72 of the elements lie on the free surface. This design acts to maximize contact response and contact deformation while maintaining a relatively low element count. The elements are 4-nodal, linear, continuum plane strain elements with reduced integration, labeled as CPE4R in Abaqus 6.8.2.

2.2.2 *Particle Packing*

The packing of particles is a crucial point of interest in discrete simulations such as MPFEM and DEM. If the initial configuration is too regular, crystalline regions can develop and cause polycrystalline phenomena such as slip planes that can greatly influence macroscopic behavior. In addition, packing methods, where material is "poured" or directionally biased, can introduce unnecessary anisotropy into the system.

The packing procedure used in this work is not exempt from the above difficulties but provides an adequate configuration for this analysis. The methodology initiates by creating a loose packing of rigid circles inside a

rectangular box. Each particle is attempted to be randomly placed at the bottom of the box. If the position is occupied, a new random location is chosen at a slightly higher position. This algorithm is executed until the box is filled with all the particles (Figure 2.2-A). After a loose array of circles is generated, the system is packed into the roll compactor through a biased random "velocity" method (Figure 2.2-B). In essence, it is a form of a classical energy minimization technique known as simulated annealing [32]. An iterative procedure is defined such that at each step, the center of every particle is assigned a new position inside a small neighborhood surrounding the current location. The new position is randomly assigned and only biased by the limits of the neighborhood (Figure 2.2-C). These limits are determined beforehand by the user and can be adjusted throughout the process to promote particle migration in any direction. This method permits particles to "jump over" adjacent counterparts while translating downward or can be used to create vertical and horizontal vibrations. The roll geometry and feed walls also constrain the velocity neighborhood and, thus, cause the particles to densify into the geometry necessary for finite element analysis (Figure 2.2-D).

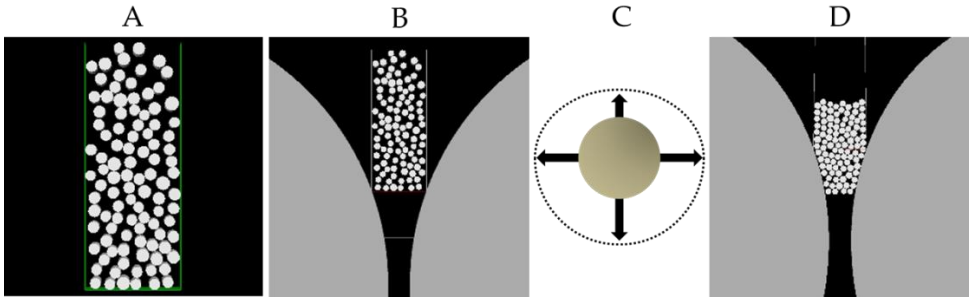

Figure 2.2 Packing procedure steps include (A) loose packing, (B) moving to roll compaction geometry, (C) application of biased random velocity, and (D) final densification

In addition to selecting the number of particles, the size distribution is chosen as a normal distribution with a specific average and standard deviation. This distribution is formulated by using the Box-Muller transform on a set of pseudo-random numbers between 0 and 1. The data is then shifted to match the custom selected average and standard deviation.

2.3 MPFEM Model of Roll Compaction

2.3.1 Model Setup

The MPFEM model of roll compaction will be executed in the explicit integration procedure of Abaqus, a commercial FEM software. Because the mechanics involve large deformations and complex nonlinear contact, the standard implicit solver is unlikely to converge upon a stable solution in a practical timeframe. In addition, analysis tools, such as mass scaling, give the explicit method an excellent advantage.

Through a Python program, the model extracts the particle positions from the packing schemes, meshes each rigid circle with the same array of nodes and

elements in a random orientation, and writes an input file for Abaqus to execute. This method is the basic execution procedure to define the geometry nodal positions of the system. In addition, all the material parameters, interactions, and analysis tools are expressed through the input file.

2.3.2 Standard System

Various computational experimentation, trials, and theoretical work have led to the creation of a standard model. This model is not an ideal system to study roll compaction, but it is a tested system that is known to compact well and reveal representative information comparable to experiments and other models. Due to the vast number of input processing parameters and the two dimensional nature of the MPFEM simulation, properties are difficult to choose in relation to each other. Every property has a dramatic effect on the compaction process as a whole and often couples its behavior with other parameters.

The entire MPFEM model can be nondimensionalized, and thus the absolute value of each particle property is not of particular importance. The ratio of elastic modulus to yield strength is one of the more applicable terms, considering it can scale with forces and torques. However, that being said, the absolute values of particle properties are based loosely on some experimental values for microcrystalline cellulose, a common pharmaceutical excipient. The powder is assumed to act as an elastic, perfectly plastic material. Extracting experimental values from El-Sakhawy's work, the particle size distribution is estimated as a normal distribution with an average radius of 5 μm and a 0.5 μm

standard deviation [33]. In addition, the yield strength is observed to be 5 MPa and density, 1250 kg/m^3. It is now assumed that the Poisson's ratio is 0.3 and that the ratio of the elastic modulus to the yield stress is 100 to 1, constraining the elastic modulus to a value of 0.5 GPa. It is worth briefly noting that the choice of density and particle radius do not greatly influence the MPFEM model. In terms of density, the model is dramatically mass scaled by orders of magnitude; therefore, the initial density is assumed to be adjusted to 1000 kg/cm^3 for convenience. The particle radius will be scaled to fit the geometry of the system. If the particle remained its "actual" size in the simulation, millions of particles would be required to fill the roll compactor. A summary of the model material properties are listed in Table 2.1.

Table 2.1 List of material properties for the standard model particle

Standard Model Particle Parameters	
Radius Average	5 μm
Radius Standard Deviation	0.5 μm
Yield Strength	5 MPa
Elastic Modulus	0.5 GPa
Poisson's Ratio	0.3
Density	1000 kg/m^3

The geometric and loading constraints of the standard model are primarily based on Cunningham's work [2] but deviate where necessary. The dimensions for the roll compactor include a roll radius of 100 mm, entry angle of

20°, and roll gap width of 1.2 mm. These values were relaxed to allow more particles into the system and easier compaction in two dimensional space. The roll radius was set to 25 mm while the roll gap width was increased to 2 mm. The important quantity described here is the ratio between the roll gap width and roll radius, named the dimensionless roll gap by Johanson [4], and it was adjusted from Cunningham's 0.012 to 0.08. Table 2.2 lists the two important geometric quantities that define the boundaries of the system.

Table 2.2 Standard model geometric parameters

Model Geometric Parameters	
Dimensionless Roll Gap	0.08
Entry Angle	20°

Loading and dynamic conditions were also obtained or approximated from Cunningham's continuum model. These parameters include a roll speed of 4 rpm (0.419 rad/s), a feed stress of 0.04 MPa, and a coefficient of wall friction of 0.4. Another important factor added is the particle to particle coefficient of friction, which is set at 0.4 as well. A summary of the loading conditions is given in Table 2.3.

Table 2.3 Loading conditions for standard model

Standard Model Loading Parameters	
Feed Stress	0.04 MPa
Roll Angular Velocity	4 rpm
Wall/Particle Coefficient of Friction	0.4
Particle/Particle Coefficient of Friction	0.4

The rolls are modeled as analytical rigid surfaces with an angular velocity boundary condition of 4 rpm. The density of the rolls is 8000 kg/m^3, and their moments of inertia are calculated by assuming solid cylinder geometries. Importantly, the feed system is modeled as a constant feed stress on the material. This assumption can be conceived as the average stress induced by a screw feeder. Finally, a maximum shear limit is proposed and valued at the yield strength of the powder divided by √3. These features describe the extent of the modeling domain.

These values for the MPFEM roll compaction model present a standard to which variations in the model can be accurately compared. With a base dataset, parametric studies are capable of being normalized and examined.

2.3.3 *Definition of Terms*

Many parameters are used to describe the roll compaction system including geometric considerations, boundary conditions, analysis terminology, and material properties. The terms are listed and defined to create a consistent framework for discussion.

The geometric and boundary conditions are best illustrated by the schematic in Figure 2.3.

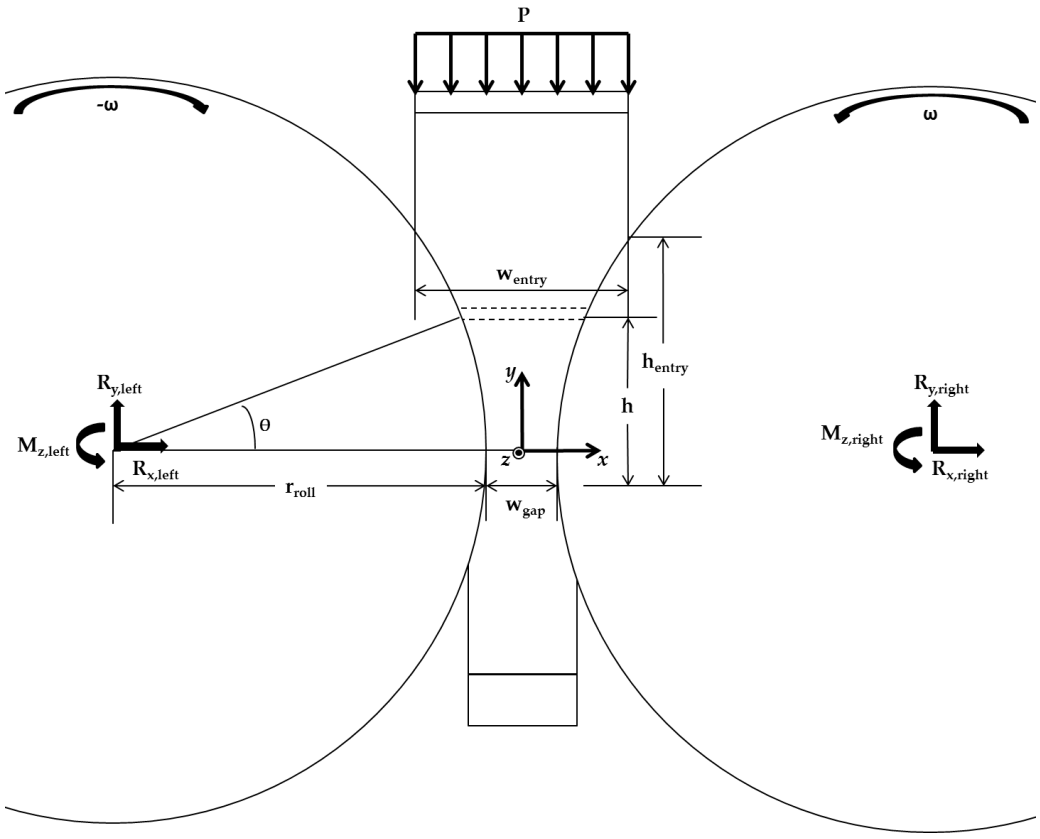

Figure 2.3 Schematic of roll compaction system with representative geometry and boundary conditions

The geometry is constrained by three primary variables, namely the roll radius r_{roll}, minimum gap width w_{gap}, and roll gap width w_{entry} at the entrance to the rolls. The entry height h_{entry} is dependent on these parameters, and either the current material angle θ or current material height h can be observed to locate the current position of a particular plane of the powder. In addition, the initial boundary conditions consist of a constant feed pressure P applied on a

deformable body above the powder and equal and opposite roll angular velocities ω. Rigid rolls and rigid walls are fixed in space, enabling reaction forces to develop. The reactions for the rolls are defined in order to construct average reaction component parameters used in the analysis. Three terms are assigned to be

$$R_x \equiv \frac{\left|R_{x,left}\right| + \left|R_{x,right}\right|}{2} \tag{2.1}$$

$$R_y \equiv \frac{\left|R_{y,left}\right| + \left|R_{y,right}\right|}{2} \tag{2.2}$$

and

$$M_z \equiv \frac{\left|M_{z,left}\right| + \left|M_{z,right}\right|}{2} \tag{2.3}$$

From this description, R_x is similar to a mean compressive force on the material and is an indicator of the pressure experienced by the powder.

The system properties must also be defined for later use. Two friction coefficients are used in the simulations, the particle to particle coefficient of friction μ_p and the particle to wall coefficient of friction μ_w, to control the contact behavior of the particles. The particle diameter $d_{particle}$ is important because it has a direct correlation with the number of particles in the system. In fact, a more significant representation is the ratio of the particle diameter to the gap width,

$$\chi = \frac{d_{particle}}{w_{gap}} \tag{2.4}$$

which essentially acts as a dimensionless particle diameter or can be recognized as the inverse of the number of particles spanning the roll gap. Other particle

parameters include the elastic modulus E, Poisson's ratio ν, yield stress σ_Y, and mass density ϱ.

2.4 Modeling Tools

2.4.1 Primary Practical Challenges

Roll compaction modeled with MPFEM becomes a highly nonlinear, contact problem with large shear and compressive deformation and involves many degrees of freedom. With the present computational technology, this effort is most likely not practically possible. However, a couple standard FEM tools and a method for addressing variable contacts render the problem approachable under a reasonable timeframe.

There are three major challenges that significantly increase computation time and hinder solution stability. The first issue pertains to the explicit integration procedure in the FEM solver. In order to ensure a stable solution in explicit analysis, a small enough time step must be chosen to guarantee stability. The stable time step is a function of the characteristic length scale (smallest dimension of all elements) and the dilation wave speed (dependent on density and the effective Lame's constants). Modeling roll compaction with MPFEM requires an extremely small time step. The second challenge to this analysis is managing the tremendous amount of mesh distortion and deformation at the contact surfaces. Without proper oversight, nodes on the edges of deformed particles may be pulled from the particle at a stress concentration and cause numerical instability. Lastly, the third issue relates to the selection of contact

pairs in the model. If contact pairs or not chosen prudently, the computation time for individual simulations can become quickly impractical. A suitable solution is presented for each of these major roadblocks and expanded in the next sections.

2.4.2 *Quasi-Static Analysis*

In the explicit integration procedure for the finite element method, a stable time step must be calculated to be sufficiently small as to guarantee that the solution does not become unstable. The condition for a time step, Δt, to remain stable is that

$$\Delta t \leq L_{min}\sqrt{\frac{\rho}{\hat{\lambda}+2\hat{\mu}}} \tag{2.5}$$

where L_{min} is the characteristic length (smallest dimension of all elements), ρ is the mass density, and λ and μ are the effective Lame's constants [34]. For an isotropic, elastic material, the denominator of Eq. (2.5) becomes Young's modulus. As a rough estimate for the time step of an ideal MPFEM simulation of roll compaction, Δt was computed to be on the order of 10^{-8}-10^{-9}. This analysis would require close to one billion increments to execute a one second simulation, which is about 3-4 orders of magnitude above Abaqus's recommendation.

Fortunately, an analysis tool, termed mass scaling, is a common and effective practice for increasing the stable time step under particular conditions. The general idea behind mass scaling is that as the mass (or density) in Eq. **(**2.5**)**

is increased by a factor k, Δt is increased by a factor $k^{1/2}$. Therefore, by artificially amplifying the mass of the system, the computational cost is reduced.

Mass scaling is a valuable means of increasing the stable time step but can only be applied to quasi-static analyses and some transient dynamic events. The focus here is placed on quasi-static analyses since roll compaction is an excellent example of this process. A quasi-static event is a dynamic event at which the material velocities are so low that the resultant inertial forces do not effectively influence the primary mechanical behavior of the system. The roll compaction process conforms to this definition because the particle speeds (often on the order of mm/s or cm/s) are not comparable to the large amount of total strain energy. When modeling a quasi-static event, mass scaling is acceptable to use providing the impact of inertia remains an inconsequential effect on the mechanical solution. The most suitable measurement tool for testing the validity of a particular mass scale is to calculate the ratio of kinetic energy to internal energy. Abaqus recommends this ratio be held under about 5-10% [34], but it is often best to define 1% as the maximum limit.

Because of the important reduction in computation time and the fact that roll compaction meets the criteria for a quasi-static analysis, mass scaling will be employed in the MPFEM model. A full analysis of the energies involved and the effects of increasing density will be discussed further in later sections.

2.4.3 *Arbitrary Lagrangian-Eulerian Adaptive Meshing*

Large shear deformations and complex contact boundary conditions cause roll compaction to produce numerical stability errors at particle surfaces from severe mesh distortion. This issue was commonly recurring in the analysis and demanded focus. One of the simplest and most effective solutions to errors from mesh irregularities is the implementation of Arbitrary Lagrangian-Eulerian (ALE) adaptive meshing. This technique is another tool supplied by Abaqus to assist in analysis work.

Typically, FEM is a Lagrangian process, in which the solver follows the spatial and temporal evolution of specific nodal points while the elemental volume comprised of these nodes remain inside the connecting limits. In an Eulerian analysis, a control volume is identified, and the rate and amount of material flow that passes through the boundaries of this volume is recorded and examined. The ALE adaptive meshing strategy combines the two procedures by allowing the material to flow through the mesh while the connectivity and elements of the mesh lattice remain unchanged. This method helps relieve heavy distortions in the mesh through readjusting nodal positions over the material accordingly.

The actual implementation of ALE adaptive meshing is straightforwardly executed in Abaqus. In its simplest form, the user chooses how many time increments elapse before the ALE adaptive meshing is reapplied, adaptive meshing frequency, and how many times the sweeping algorithm is performed

per each adaptive meshing, adaptive meshing sweeps. The number of adaptive meshing sweeps was determined to be adequate at the minimum (one sweep per remeshing), and a brief analysis was undergone to monitor the influence of adaptive meshing frequency on CPU time. An example of general behavior is shown in Figure 2.4.

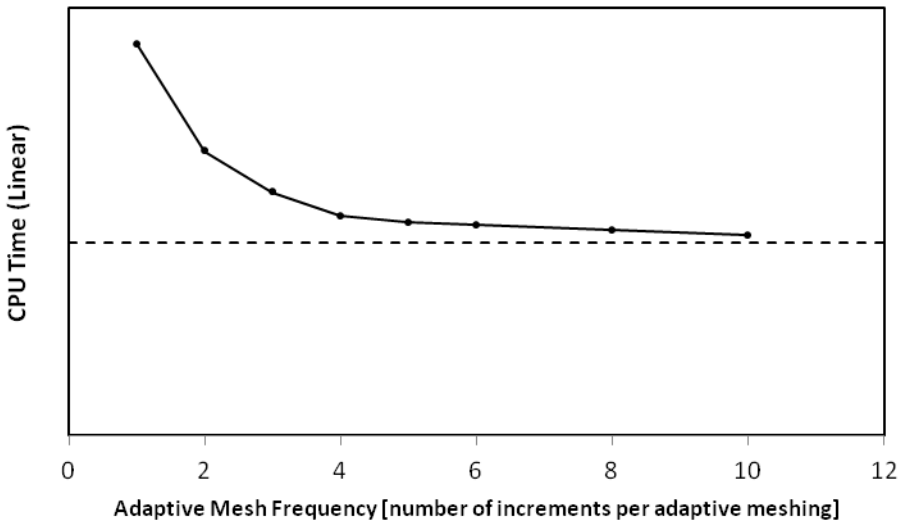

Figure 2.4 General dependence of CPU time on frequency of adaptive meshing in MPFEM roll compaction

This trend revealed that a frequency of 5-6 increments was not likely to critically increase the overall CPU time of the analysis but would, however, provide a satisfactory frequency of adaptive meshing.

2.4.4 Contact Detection and Definition

Contact mechanics is an important topic in modeling discrete behavior. In DEM, assumptions are devised to generate a contact interaction law and it

often indirectly governs the particle micromechanics. On the other hand, a technique such as MPFEM handles contact interactions much more naturally. Finite volumes, contact areas, and surfaces already exist, and their coordinates are known. The exact clearances and overclosures can be determined at each time step, and the amount of overlapping areas is readily available.

However, a great expense arises from the accurate depiction of surfaces. The procedure must track the various deformations and displacements in the model and determine the most likely regions of contact. Contact pairs of possible interacting surfaces are defined a priori by the user. Then, individual nodes of the slave surfaces must be checked for contact against that of the master at each time step, and if successful, computations must be performed. With as many surfaces as particles, an MPFEM model demands a computationally exhausting workload from contact tracking algorithms. It becomes important to wisely select contact pairs. For example, in Figure 2.5, it is severely unlikely that a particle from 'Zone A' would ever come in contact with a particle from 'Zone B' throughout the analysis.

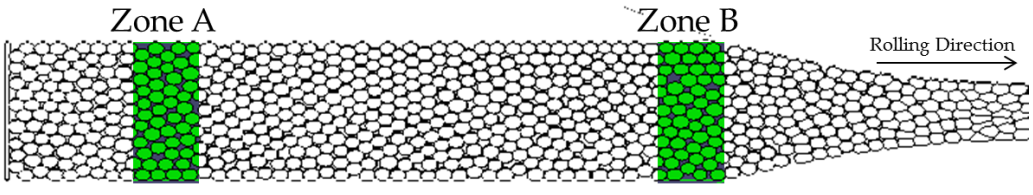

Figure 2.5 Two zones in roll compaction that are unlikely to interact throughout the analysis

Thus, a more reasonable choice is to define contact pairs between particles whose surfaces lie within a certain distance of each other. Every particle is defined to have a contact range measuring several particle radii in length. The contact range develops an annulus around the particle's surface (Figure 2.6-A), and if a portion of another particle's surface is located in this region, it is defined as a potential contact. With this designation of contact range, a plot is shown in Figure 2.6-B to demonstrate the general trend observed between CPU time and contact range.

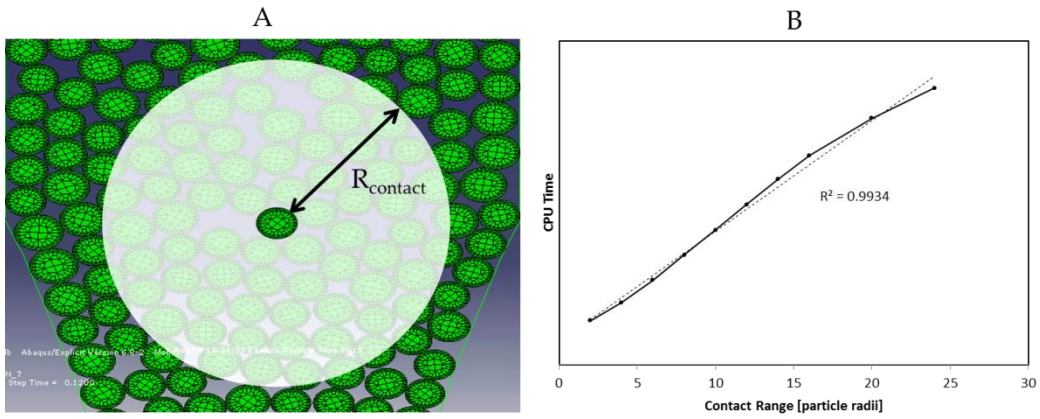

Figure 2.6 (A) Contact region defined around each particle and (B) general dependence of CPU time (linear axis) on increasing contact range

It is apparent that enlarging the length of the contact range can considerably increase the total simulation times for MPFEM roll compaction, and it emphasizes the importance of optimizing this parameter.

In Procopio's work, the contact range was 6 to 8 particle radii in length and predefined at the onset of the simulation [29]. However, this contact pair

assignment was designated for die compaction. In the case of roll compaction, the non-uniform flow patterns and intense shearing near the rolls create difficulties for the static contact range. It was found that particles well outside the cautiously defined range were capable of shuffling into the region and interacting with undefined partners. Eventually, an impractical expansion of the contact range was demanded by the dynamics of the system.

Because of the necessity for reducing the CPU time of the analysis and the flaws in predefining a contact range, an incremental approach to detecting and defining contact pairs is implemented for the roll compaction model. It is proposed that a more time efficient means of locating potential contacts between particles is achieved by splitting the model into temporal divisions and utilizing a small, but variable contact range for each model division. The basic methodology includes submitting the simulation with a small contact range (normally 2-3 particle radii), stopping the analysis after a particular time step, reading the output database to extract current particle locations, updating the contact pairs, restarting the analysis, and then repeating the process until the total simulation time has elapsed. This process is automated through the Python scripting framework in Abaqus, and the models are typically broken into 10 – 25 divisions for efficient analysis. The procedure is concluded to be effective and resourceful and is, therefore, utilized in the MPFEM roll compaction simulations.

2.5 Steady State Analysis

2.5.1 Introduction to Steady State

Most processing techniques will eventually reach a mechanical (or thermal, etc.) state at which the variables of the system become constant with respect to time. For example, feeding a uniform, continuous amount of material through a roll press will cause the reaction forces and torques on the rolls to become stable after a given elapsed time. In addition, the product strip thickness and density may also become consistent or slightly oscillatory. It is at the moment that the temporal derivatives of the internal variables of the system become zero that the system is said to have reached steady state. Because the inputs and outputs remain constant at steady state, it is important to detect the onset. At this point, direct comparisons can be made between other systems in steady state, and experiments can be performed. Quasi-static simulations are often terminated once steady state is determined to have been reached because new information is unlikely to be observed.

2.5.2 Transience and Steady State Detection

Before a steady state condition is achieved, a transient zone is present and controls the behavior of the system. Over time, the transience is smoothed out of the process and only spatial relations remain. Examples of transient regions are depicted in Figure 2.7.

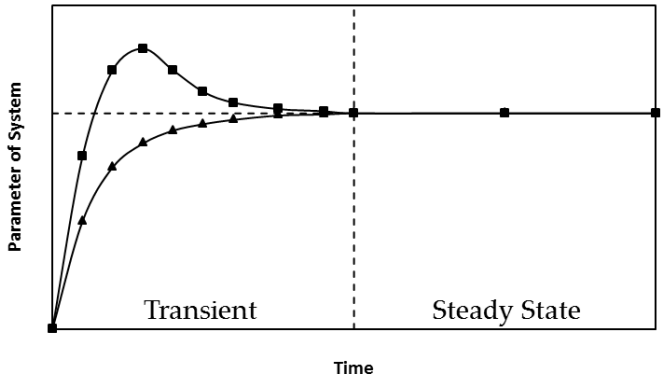

Figure 2.7 Transient regions moving into steady state over time

One of the goals of this work is to attain steady state conditions for parameters of the roll compaction system to justify accurate comparisons between input conditions. A detection of these processes can sometimes be inferred when a plot with time converges to a plateau, resembling that of Figure 2.7. However, experimental data has displayed many oscillatory motions occurring during roll compaction in the past [20] so a full steady state condition may be difficult to achieve or precisely define. This struggle is especially prevalent when even maintaining a simulation for a long period of time in the transient zone is computationally exhausting. In theory, it is impossible to achieve a true steady state for an experimental particulate method because the incoming geometry of the system constantly varies in time. This reality is exacerbated with a finite system of particles because the statistical difference between configuration geometries is increased. Thus, a steady state analysis must be considered from a time averaged viewpoint.

CHAPTER 3: RESULTS AND DISCUSSION

3.1 Convergence and Mass Scaling

3.1.1 Convergence as a Validation Method

There are many features of the MPFEM roll compaction model that must reach some level of convergence to become most useful. Model parameters such as total roll force, total roll moment, relative density, and strip thickness are expected to develop as constants of time during a roll compaction process. As compaction begins, the system enters into a transient state and attempts to reach temporal independence. The onset of steady state must then be characterized as a convergent condition with respect to time, where the rates of parametric changes meet stable criteria. For example, the roll compaction system could be considered to be in steady state when the total force on the rolls does not vary greater than 5% from a past measurement. Similar criteria could also be mapped to a sinusoidal function to determine when steady state oscillations emerge.

Besides application to steady state analysis, achieving convergence becomes important in mass scaling, particle quantity, and mesh optimization. To some extent, Procopio justified the use of this mesh for a system such as roll compaction [30]. Testing both of the other aspects of the model is pertinent to the solution accuracy but requires demanding amounts of CPU time to properly study.

3.1.2 Mass Density

Monitoring the effects of mass density is an important task while applying mass scaling techniques. As discussed earlier, increasing the mass of the system by a factor of k will typically increase the stable time step by a factor of $\sqrt{k}$. However, when the mass is scaled too drastically, inertia effects begin to dominate the equilibrium solution. The appropriately level of optimization is judged by the ratio between kinetic and internal energy, and the value is recommended to be maintained below 1-10%.

For this particular study, added caution was practiced while performing mass scaling, due to the nonuniform nature of the micromechanics of the system, e. g., the substantial differences between the slip, nip, and extrusion zones. In certain regions of the process, rearrangement and rotation are the prevailing mechanisms of motion and can be considered inherently kinetic activities. These locations are regions of attention because mass scaling may greatly diverge their solution. Only small deformations occur in these areas, allowing the kinetic energy to become a sizable percentage of the internal energy. A range of material mass densities are investigated to determine a suitable value for future simulations, and the results are displayed in Figure 3.1. In the MPFEM roll compaction simulation, a large percentage of the trial time demonstrates the transient state of the system. Compaction does not immediately occur until a sufficient number of particles progress through the rolls and develop initial stresses and resistance networks in response to the boundary conditions. This

temporary stagnation yields relatively high amounts of kinetic energy dominating the system.

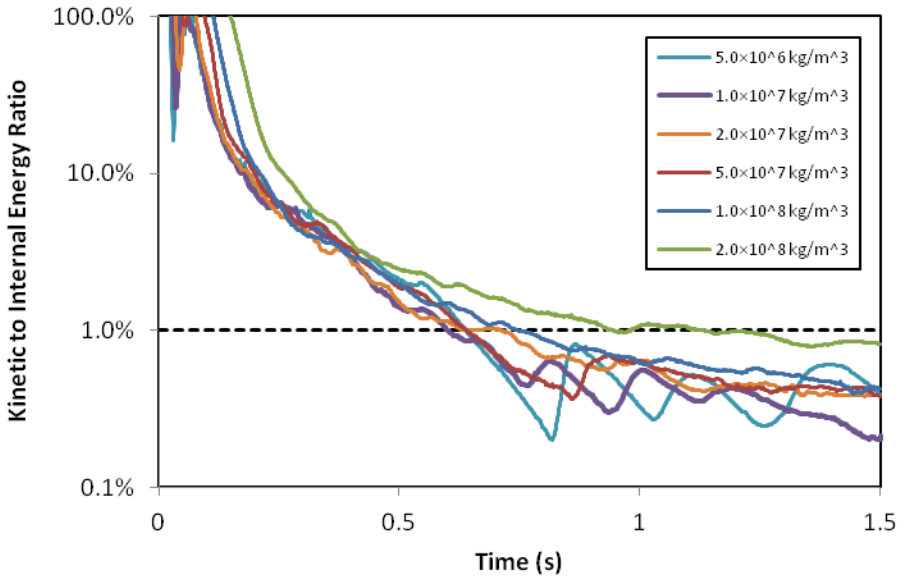

Figure 3.1 The kinetic energy to internal energy ratio for various powder mass densities throughout the course of the simulation

However, the kinetic influence is quickly dispersed, even in the transient zone, and the ratio is maintained below 1% for the remainder of the analysis. The density of the particles for the standard model is selected to be 1.0×10^8 kg/m^3 from the results of Figure 3.1. This specific value efficiently compromises between solution accuracy and CPU time minimization.

The effects of mass scaling density can also be judged on the basis of output parameters of the system. With a proper scaling, performance should be generally unchanged as density is decreased. In Figure 3.2, the average roll reaction force is observed in the x direction. A direct correlation between the roll

force and the effect of density is not clear except at the very early stages of the simulation where loading first occurs and no compaction exists. The general behavior of the system stays unaffected through various densities while the force magnitudes float within the range of error and system noise. The lack of a clear steady state prevents a true convergence analysis, but some features of convergence may be observed in the early stages of the simulation. A convergent increase in compressive force is seen for decreasing mass scaling factors in the range $t < 0.15$.

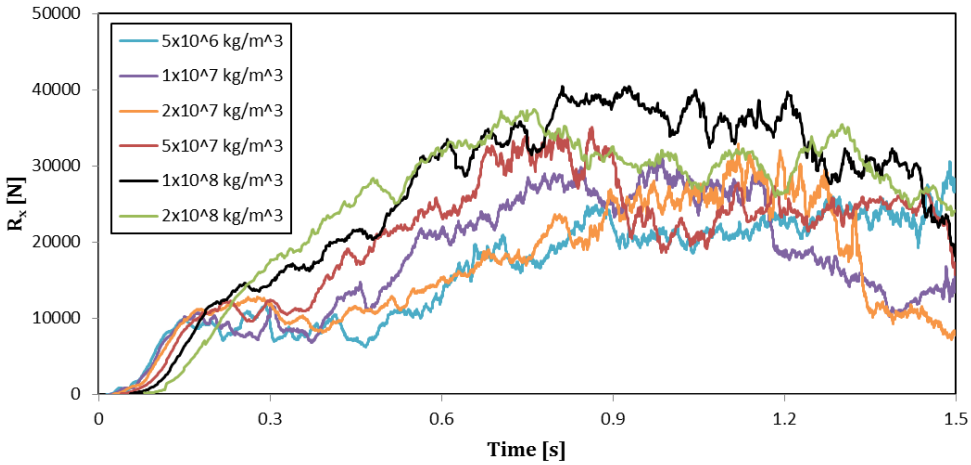

Figure 3.2 Average roll reaction force in X with various densities

3.1.3 *Particle Count*

The quantity of particles used in the simulation not only steeply lengthens CPU time but also demands large amounts of RAM and hard disk memory. Therefore, unnecessary increases in the number of particles must be avoided at the aim of practicality. On the other hand, a true roll compaction

process involves millions of particles and must be modeled with a representative amount of degrees of freedom. This issue presents a difficult tradeoff for MPFEM and needs to be addressed in some detail.

A convergence study in particle count is presented by Procopio for multi-axial die compaction [29], but an equivalent study may be difficult to replicate for roll compaction. In die compaction, the primary source of error in low particle quantity systems is the wall effect. That is, particles near a rigid surface will be unable to pack as well as their bulk counterparts, promoting larger deformations in these regions and inducing macroscopic rigidity. To relieve the effect, the bulk particle count is increased until the error is adequately diminished. In the case of roll compaction, a wall effect also exists at the rigid surfaces. The most vulnerable area for this phenomenon to obstruct is found at the roll gap where the two rigid rolls are nearest. Here, a sufficient number of particles must fill the gap to mitigate the wall effects from both sides.

A convergence study is presented for the particle count in terms of a quantity, referred to as χ, defined as the ratio between the average particle diameter and the roll gap width (inverse of the number of particles that can be aligned across the gap). Explicitly,

$$\chi = \frac{d_{particle}}{w_{gap}} \tag{3.1}$$

Decreasing the χ, in essence, forces the particles to shrink relative to the geometry of the system. In order to maintain a roll compaction system with a

smaller χ, equivalent geometry, and conserved mass of material, the particle quantity must be increased. Therefore, a strict inverse relationship is fixed between the χ and the particle count.

Analyzing similar systems with different particle sizes and counts, it is possible that convergence will occur for a limiting χ. This investigation is performed in Figure 3.3, where the average roll force in the x direction is observed.

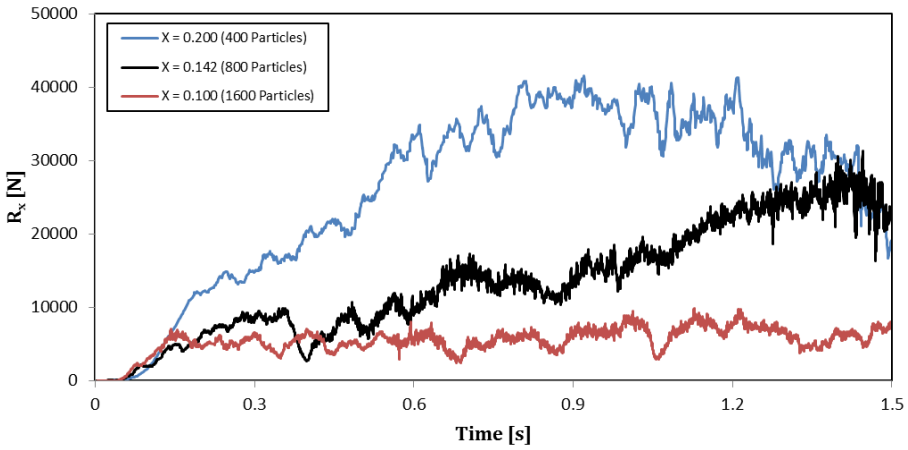

Figure 3.3 Average R_x on rolls for various χ

The curves suggest possible convergence for $\chi = 0.2$ and $\chi = 0.142$, but it is unclear whether either will converge to the other system. More interesting to note is the trend in the transient zone for R_x. This parameter is an indirect measurement of how well the material is compacted; for large R_x, the material is pressed between the rolls at a high stress in the x direction. Therefore, Figure 3.3 shows that the material is well compacted with a larger χ. There may be

multiple explanations for this result. Firstly, it could be an outcome of wall effects. Very few particles can align across the roll gap width with the larger χ, causing a worst case scenario for avoiding dominant wall effects. Another explanation for weak compaction with small particle diameters is that a stress chain development becomes more difficult. For compaction to occur in a discrete analysis such as MPFEM, the load must be transmitted through a network of particles to each boundary surface. For small χ, the chain carrying the forces has many degrees of freedom, and thus breaking and rearrangement of the chain becomes a more probable event than compaction through the network. On the other hand, it is difficult to avoid compaction through stress chains when there are only several particles across the χ. This scenario is more likely to occur for cohesionless particles. In that sense, higher coefficients of friction might have reduced this transient zone, enabling a better depiction of convergence across all domains.

3.2 Parametric Studies

3.2.1 Feed Stress

As discussed earlier, the feed system of the MPFEM model consists of a constant pressure distributed over a surface boundary above the particles. This simplification is analogous to averaging the pressure applied by a screw feeder in a commercial roll compactor. The effects of the feed stress magnitude is explored in most roll compaction models and is directly related to the pressures

experienced by the resultant rolled material. A similar analysis is shown in Figure 3.4 using the MPFEM model.

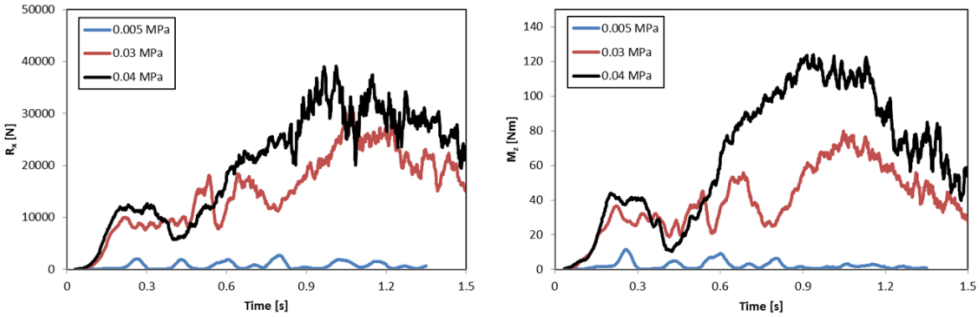

Figure 3.4 Average roll reaction forces and moments for various feed pressures

The feed pressure is a crucial part of the rolling compaction process. The compactor supplies a mechanical advantage, proportional to the feed stress and dependent on other factors such as material properties. If the supplied force is not large enough, the material cannot be rolled. This situation is the case for $P = 5.0x10^4$ *MPa* and, consequently, the simulation was unable to complete (Figure 3.4). The effect of variation in feed pressure magnitude is illustrated through the plots of Figure 3.5.

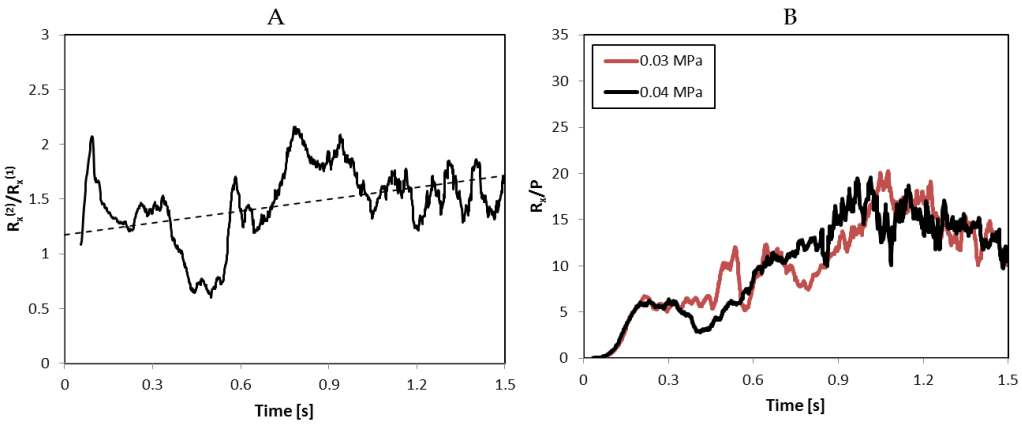

Figure 3.5 (A) Roll force reaction ratio from P = 0.04 MPa and P = 0.03 MPa and (B) Normalized roll reaction force at different feed pressures

The ratios between the reaction forces of two separate studies of feed pressure show that the quotient remains relatively unchanged. Furthermore, the average ratio calculated to be approximately 1.48, which is near the ratio of the feed pressures themselves. Johanson's model demonstrated the proportionality existing between feed pressure and induced roll pressure [4], which is analogous to this dataset. When the reaction force is normalized by the feed pressure (Figure 3.5-B), very little variation is observed between the two systems. The feed stress also greatly controls the predensification process. When larger pressures were attempted, particles were plastically deformed upon entrance into the nip zone.

3.2.2 *Roll Speed*

The roll angular velocity is an important processing parameter that can be set by a roll compactor user. In the standard MPFEM model, the value of 4 rpm was selected to implement in the simulations based on past experiments and

models. The effect of doubling the angular velocity is analyzed by running a simulation at half the total time, but double the roll speed. Due to the quasi-static nature of the system, varying a dynamic parameter should not significantly hinder the equilibrium solution. This consistency is observed in

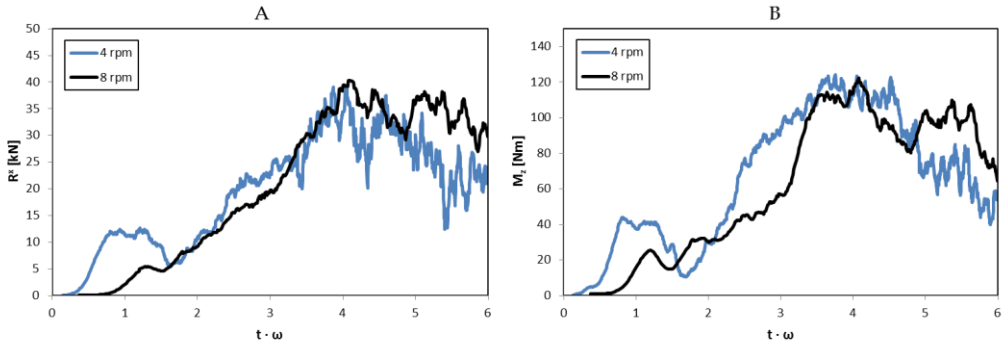

Figure 3.6 Effect of doubling roll angular velocity on averaged (A) reaction forces and (B) moments

Doubling the angular velocity of the rolls produces a fairly equivalent response from the system compared to the initial state. The largest variation arises at the early stages of compaction where the kinetic energy is dominant. This outcome is expected and confirms the quasi-static assumption.

3.2.3 *Friction*

The frictional interactions between particles and boundaries are macroscopically modeled through various assumptions and experimental calibration. In MPFEM, friction is handled naturally as a micromechanical contact criterion at each particle's surface and may give a more accurate depiction of tribological behavior. Two major sources of friction are present in a roll compaction system, which include particle to particle friction initiated at the

interfacial boundaries of particle contacts and particle to wall friction occurring between the roll and particle surfaces. A study of the limitations of the two coefficients of friction reveals that each is a necessary parameter for successful compaction. When the either wall or particle coefficients of friction become too large, the particles are unable to rearrange and expand to the spatial freedoms of the system. This restriction leads to a jamming of the simulator roll press or overcompaction, extreme densification, of the material. However, with very low coefficients of friction, the powder is capable of avoiding significant compaction by readjusting and flowing through the system. An illustration of the compaction zone in a frictional space is presented in Figure 3.7. A full probing validation of the boundary regions was not performed; the graphical lines are for conceptual purposes. In addition, the compaction region is able to mutate for various mechanical and geometrical states of the system.

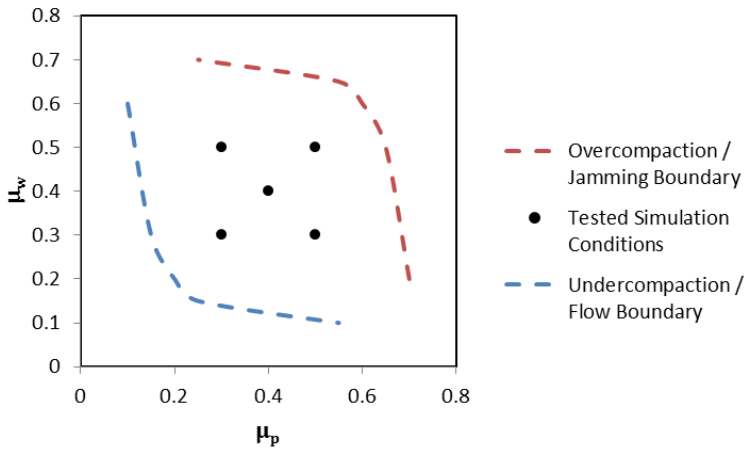

Figure 3.7 General boundaries of the coefficients of friction determine whether a material can compact through a specific roll press

The five points shown in Figure 3.7 correspond to performed simulations at variable tribological conditions in the compaction zone. Friction generally assists the compaction of particles by hampering range of motion and forcing flow in a steady manner. In addition, large frictional forces can cause substantial local shear deformations. The results in Figure 3.8 reflect this general friction analysis and emphasize the importance of understanding the role of friction during roll compaction.

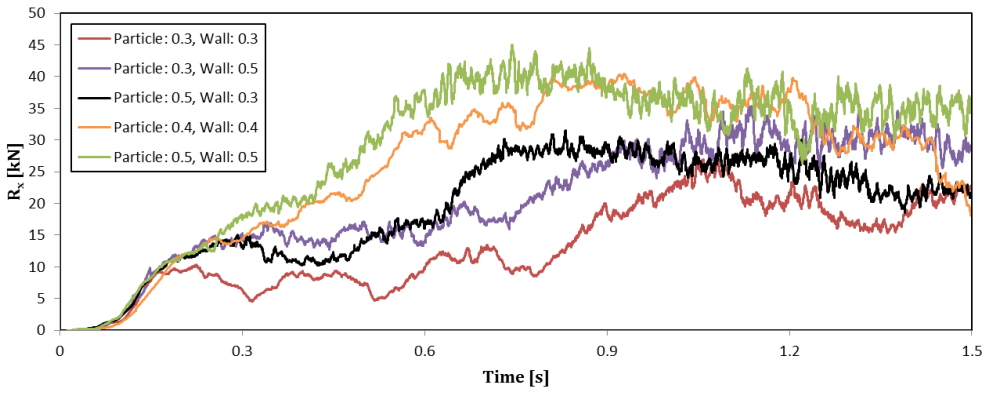

Figure 3.8 Average roll reaction force for various combinations of wall/particle and particle/particle coefficients of friction

3.3 Shear Bands

3.3.1 Shear Banding

Shear bands are zones of dramatic shear deformation that primarily develop in ductile and porous materials, which permit plastic flow before final failure. Certain loading and boundary conditions are required for this type of behavior to guarantee that enough freedom of motion is available to displace the

mass. A classic case of shear banding occurs when a cylindrical material, unbounded in the radial direction, is subjected to pure compression. The shear deformation will cause angular plastic flow, breaking the material into "bands". Studies have been performed to show the development of shear bands in granular media [35], Figure 3.9.

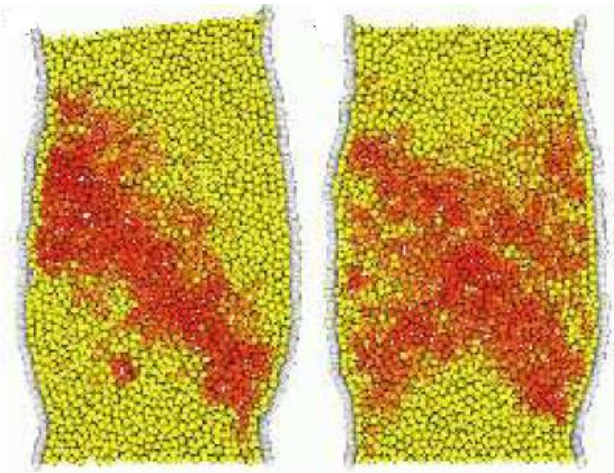

Figure 3.9 Depiction of shear bands from DEM simulations of granular media [35]

This same phenomenon can be seen at the micromechanical level of powder roll compaction. As particles are drawn through the rolls, the geometric constraints promote velocity vectors to develop at an angle relative to the rolling direction. Thus, a particle band shears across a layer of another band until the deformation is interrupted. This flow pattern occurs numerous times over the course of the roll radius and causes a nonuniform distribution of velocities. The velocity field perpendicular to the rolling direction is shown in Figure 3.10 for a particular time increment at standard conditions and $\chi = 0.1$ (1600 particles)

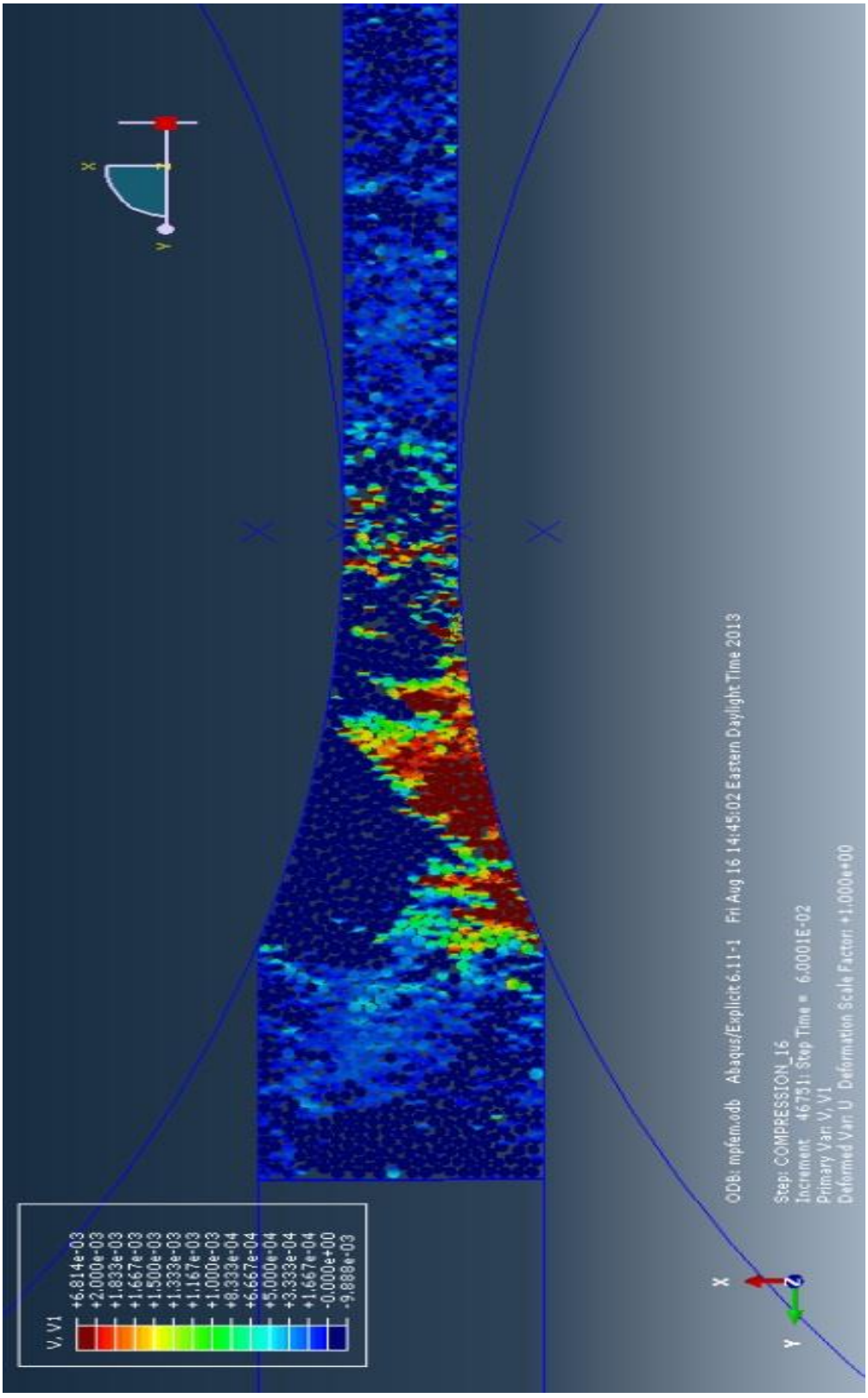

Figure 3.10 Velocity distribution in x direction depicting multiple shear bands forming with $\chi = 0.1$ (1600 particles)

3.3.2 *Deviation from Base Velocity Field*

Another procedure for illustrating the evolution of shear bands is to subtract a base velocity field from the particles' motion. This method entails extracting the coordinates and velocity components from each particle and comparing it to an assumed regular flow. It is analogous to a nonaffine motion analysis for die compaction. However, the affine motion is not as easily obtained from the boundary conditions in roll compaction, and thus assumptions must be developed. The velocity field in Figure 3.11-A is derived from an MPFEM roll compaction simulation while the velocity field in Figure 3.11-B is based on assumed motion through the geometry.

Figure 3.11 (A) Actual particle coordinates and velocities from simulation compared to (B) assumed velocity field for $\chi = 0.2$ (400 particles)

The base velocity is restrained and calibrated to the input and output velocity of the actual system and interpolates the remaining field linearly through either direction. As the velocities approach the rolls, the motion is assumed to become tangent to the boundary. The linearity assumption is a simple approach to building a comparison field and is not far from reality. Measured flows across the x and y directions in previous simulations have

shown that the velocity components vary approximately in this manner. The base field can now be subtracted from the actual field, demonstrating the deviation from the assumed motion, Figure 3.12.

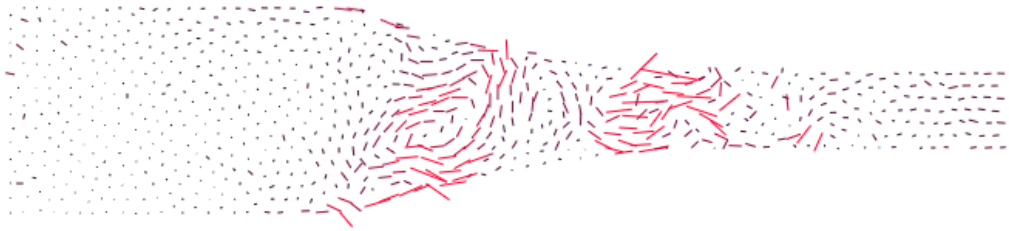

Figure 3.12 Deviation from base velocity field showing indication of shear bands for $\chi = 0.2$ (400 particles)

The deviation field depicts a zigzagged flow through the geometry, indicating the existence of shear bands on each side of the interface. The temporal evolution of shear bands is fairly sporadic and can be visualized through an animation of the deviation field or a series of images shown in Figure 3.13. The shear bands can reverse directions and move throughout the length of the rolls during compaction.

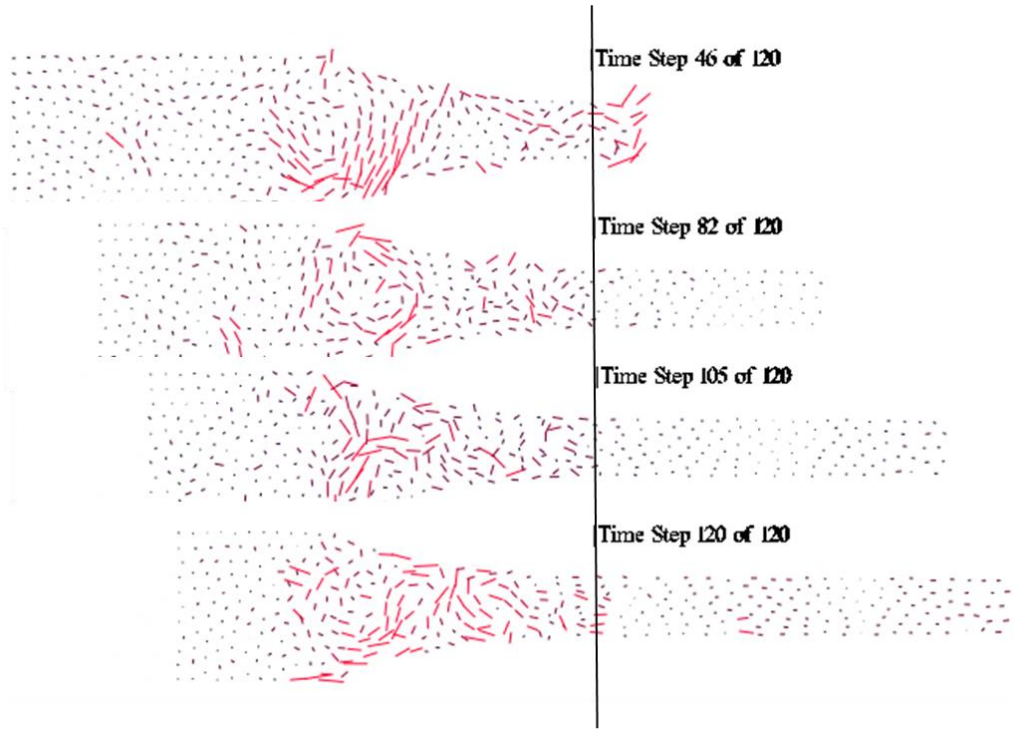

Figure 3.13 Series of time step images indicating the temporal evolution of shear bands

3.3.3 Gradient Field

The deviation field reveals the irregular motion of particles advancing through the roll gap and implies the existence of plastic shear bands. The boundaries of these bands can be highlighted further by recognizing the large change in velocity across these borders. Therefore, observing a spatial gradient of the velocity field enhances this feature. The gradient field implemented in this work is not a true spatial gradient but will be defined as the sum of the change in each particle's velocity component normalized by the *total* distance between particles. Essentially, the gradient is given a magnitude and orientation for each pair of particles, *i* and *j*, where the vector is expressed by

$$\nabla\vec{v}_{ij} \equiv \frac{v_{ix} - v_{jx}}{\sqrt{(v_{ix} - v_{jx})^2 + (v_{iy} - v_{jy})^2}}\hat{x} + \frac{v_{iy} - v_{jy}}{\sqrt{(v_{ix} - v_{jx})^2 + (v_{iy} - v_{jy})^2}}\hat{y} \qquad (3.2)$$

where v_{ix} and v_{jx} are the x-components of the velocities for particles i and j, and v_{iy} and v_{jy} are the y-components of the velocities for particles i and j. This definition takes a number of particles N in a discrete field and computes N^2 gradient points. The total amount of calculations is reduced to much less than N^2 by choosing to only determine the velocity gradient for particle pairs that are near each other. The gradient field is plotted in Figure 3.14.

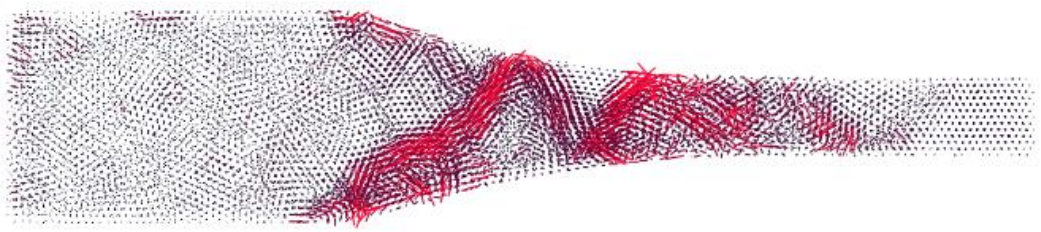

Figure 3.14 Gradient of velocity field for a particular time step for $\chi = 0.2$ (400 particles)

The boundaries of the shear bands are significantly emphasized in this type of illustration, and the existence of bands is even observed within the nip region. This analysis demonstrates a very asymmetrical behavior that emerges naturally in a powder material undergoing roll compaction. The acknowledgment of this motion raises attention to velocity assumptions when modeling a roll compaction system. Planes of the material not only no longer remain plane but also lose symmetry as they pass between the rolls.

3.4 Particle Shape

3.4.1 Shape Classification

Particle shape controls many aspects of the local mechanical properties of the system including relative density, packing, anisotropy, contact area, particle rotation, and particle velocity. A unique benefit of MPFEM is the ability to naturally account for changes in particle morphology, the only requirement being an initial mesh transformation. To explore the implications of morphological variation, three shapes are generated and simulated at equivalent conditions. The surface-biased mesh fashioned for the circle is mapped onto an ellipse (aspect ratio = 2) and a hexagon for simplicity, shown in Figure 3.15.

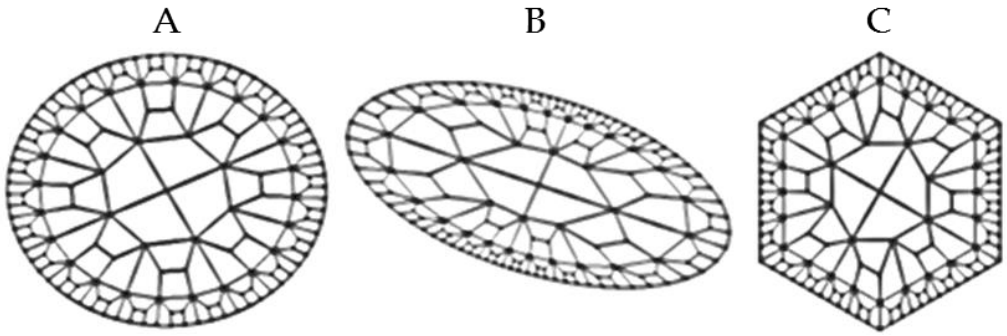

Figure 3.15 Particle meshes for (A) circle, (B) ellipse with aspect ratio of 2, and (C) hexagon

These three shapes are chosen to exemplify near extremes in morphological behavior based on the particle shape classifications of Cho et al. [36]. In that work, shape was primarily described in terms of *sphericity* and *roundness*. The

graphical table in Figure 3.16 illustrates examples of particles with an encompassing range of sphericity and roundness values.

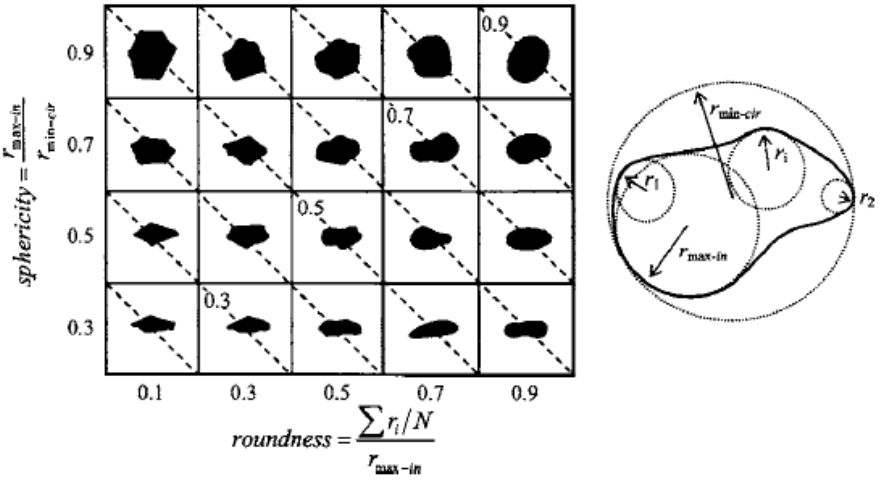

Figure 3.16 Particle shape determination - sphericity and roundness chart [36]

Sphericity is quantified as the ratio between the radius of the largest possible inscribed sphere (or circle in 2D) and the radius of the smallest circumscribed sphere. Roundness is the ratio between the average radii of spheres needed to define the surface and the radius of the maximum inscribed sphere. A circle yields a maximum value of 1.0 for both qualifications while a hexagon and ellipse are classified as low or mid ranged shapes in terms of sphericity and roundness, respectively. The distinctions between these morphologies offer a glimpse into the general behavior of any particle shape factor.

3.4.2 *Shape Effects*

The circle, ellipse, and hexagon are tested under the standard conditions introduced earlier, and each shape's area is adjusted to preserve the total mass of the system. The size distribution is also maintained. Many characteristics of the morphological effect can be immediately seen in the typical roll reaction force curves, Figure 3.17.

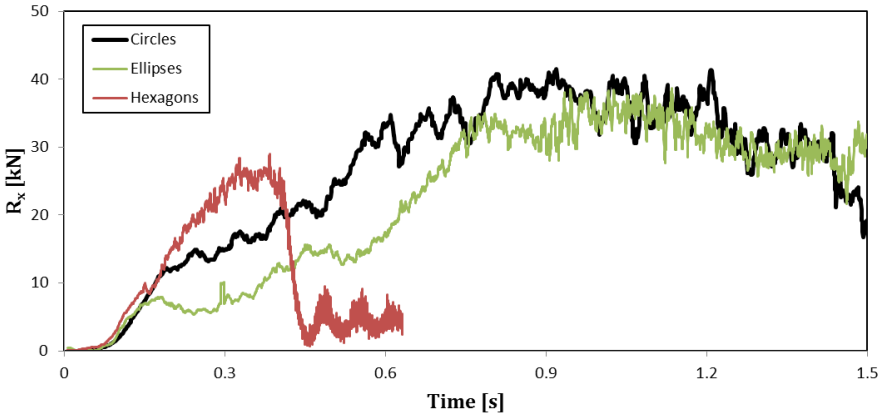

Figure 3.17 Average roll reaction force in X direction for various particle shapes

The compressive force develops at different rates according to the particle shapes' influence. For the case of hexagons, mechanical interlocking emerges very quickly, restricting rearrangement and assisting material directly through the roll gap with minimal deviation. This immediate compression constrains local rotation and displacement even further until the roll compactor "jams" and the simulation fails. The ellipses behave in a contrary manner; rotation and displacement are promoted as the particles progress through the rolls. An

explanation for this difference depends on the dramatic change in anisotropy of the system, from an initial packing oriented perpendicular to the rolling direction to a rotated arrangement oriented along the rolling direction. The large movements mitigate the compaction process by diverting energy towards inducing local motions.

A closer analysis of the ellipse simulations reveals the prominent variation in particle orientation arising at the entry angle. Estimations of the deformed and undeformed ellipse orientations are computed and illustrated as a discrete field in Figure 3.18.

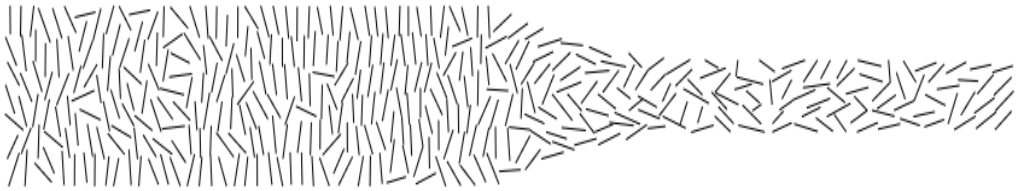

Figure 3.18 Orientation field for a system of ellipse particles during roll compaction

Initial particle packing methods lead to highly anisotropic systems when applying shapes with large aspect ratios. Avoiding this issue is often difficult and requires more sophisticated packing schemes that may not eventually reflect reality. The emergence of anisotropy above the rolls in Figure 3.18 is a probable scenario and influences the compaction behavior. As the material approaches the roll, rotation occurs very quickly at the roll surface to orient the particles tangentially. This action introduces free volume in the slip and nip regions that

is mostly easily occupied by rigid rotations of adjacent particles. A quantification of each ellipse's orientation is calculated by determining the angle between the major axis and the x direction. Averaging this orientation angle over the rolling direction at the discrete locations yields a detection of the change in anisotropy, Figure 3.19.

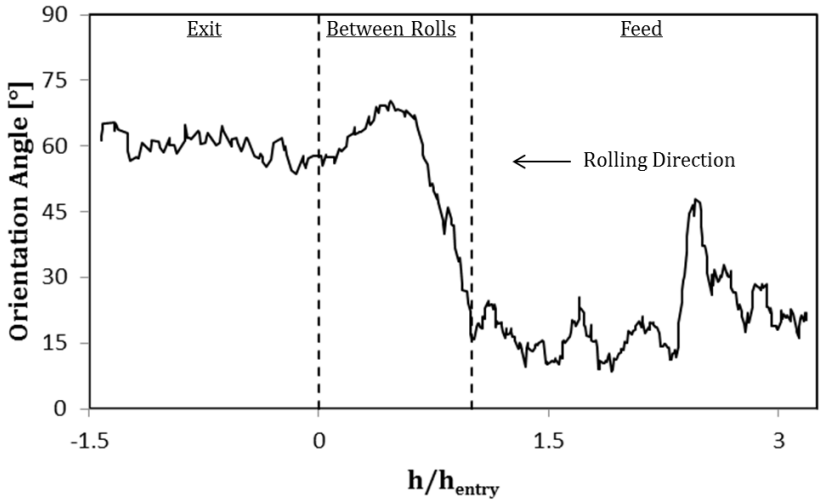

Figure 3.19 Orientation angle of ellipses through rolling direction

Before entering the rolls, the average orientation angle of the particles is approximately 20°. This value greatly increases through the compaction process and remains at about 60° after exiting the rolls. The behavior is a product of the geometric boundary conditions, which opens regions of free volume and activates local degrees of freedom.

With a large shift in anisotropy, other parameters such as porosity become affected. Relative density is not easily managed in two dimensional

space so an analysis of bulk density, or area density, is implemented to observe variation in porosity. The initial densities after packing for the circle, hexagon, and ellipse are about 80%, 82%, and 84%, respectively, and are recognized as large percentages compared to experiments due to the two dimensional nature of the packing. The application of the feed pressure marginally increases these values before the material contacts the rolls. For ellipses, the alteration in particle orientation results in a substantial drop in bulk density near the slip region where rearrangement and rotation is at a maximum. The full profile of bulk density along the rolling direction is displayed in Figure 3.20.

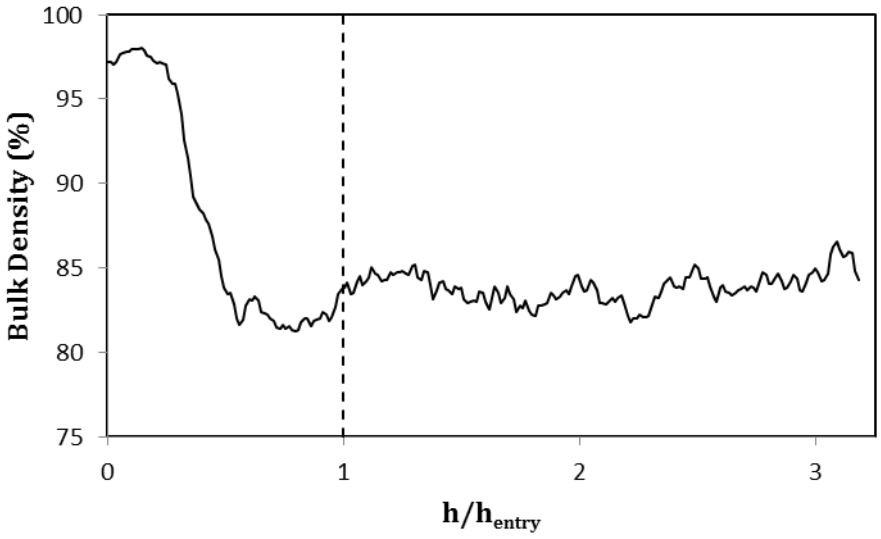

Figure 3.20 Bulk density profile along rolling direction for ellipse-shaped particles

For circles and hexagons, the response does not decrease to the same degree as that of the ellipses in the slip zone. The difference can be again attributed to the

large rotation of particles in this region. The other two shapes show similar behavior, and both develop a slight reduction in bulk density around the entry point. However, the drop may have more likely arisen naturally from random packing in these cases, Figure 3.21.

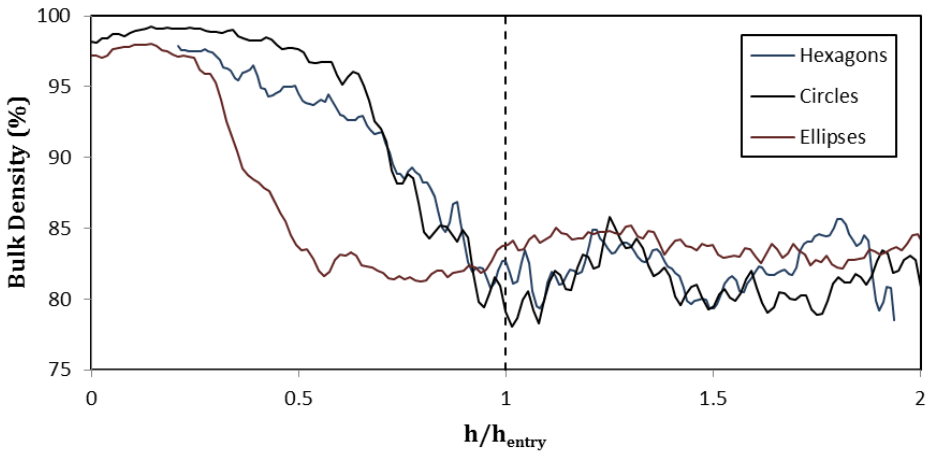

Figure 3.21 Bulk density profile along rolling direction for various shapes

These studies of particle morphology demonstrate the caution required when modeling a roll compaction process with discrete spheres or with continuous media. Even by observing only two possible shapes, irregular behavior is seen in the form of jamming, pressure variation, and bulk density abnormalities. In reality, particles exist at much more extreme geometries, e.g., very rough, asymmetrical surfaces and large aspect ratios. Particle size distributions can also couple with these effects. Shapes with low roundness create situations of mechanical interlocking and high friction that lead to large increases in compaction. The hexagons and circles were simulated at equivalent

conditions yet the hexagons compressed much quicker and ultimately jammed the system while the circles regularly progressed through the rolls. In addition, contact area is influenced by particle geometry. Ellipses avoid excessive contact with neighbors in the slip zone through rotation and rearrangement, and circles move in shear bands destroying interactions with adjacent particles. These motions can motivate poor cohesion and binding capabilities in the material and diminish properties of the resultant product. On the other hand, rough surfaces that promote interlocking, those of the hexagons, may provide the opposite effect. With its influential role in altering macro and micro scale mechanical behavior, particle shape must be considered a significant parameter in a roll compaction system, requiring careful examination during analysis.

3.5 Steady State

3.5.1 Challenges in Achieving Steady State

When studying roll compaction, it is important to attain a steady state in order to justify meaningful comparisons across instances of variation in the operating conditions. An open question remaining throughout the MPFEM analysis deals with deciding whether steady state was achieved. The appropriate method of determination must show the time independence of the parameters of the system. However, enough natural variation may exist to conceal certain features of the steady state. Particular responses of the mechanics, such as force measurements, contain oscillatory signals with no

apparent inherent frequency. This same behavior is seen in the DEM simulations, shown in Figure 3.22, where sporadic 20-40% oscillations develop.

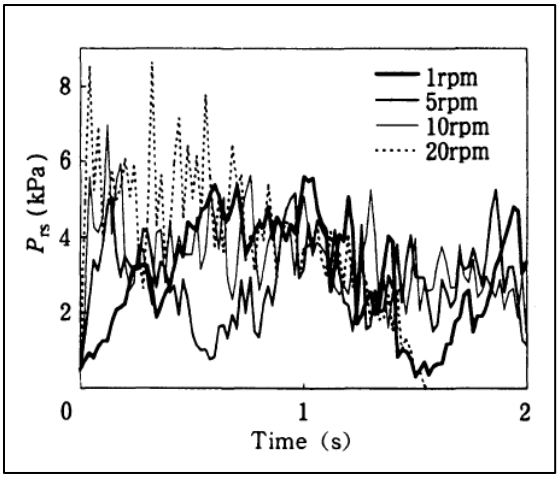

Figure 3.22 Time variation of pressure at the point of maximum mean pressure on the roll surface [37]

Furthermore, raw data from experiments shows sensor noise with similar levels of deviation and creates complications for attempts to control the output properties. Observing the average force in the MPFEM simulations may not serve as the best and only means of determining a steady state condition. The pressures experienced on the roll surfaces are subject to fluctuations emerging from numerous factors including the discrete nature of the system, deviatory velocity effects such as shear bands, numerical noise, packing biases, particle rotation and shape influences.

Thus, a better depiction of steady state may be found by analyzing other global parameters such as the velocities of the feed and plug along the roll direction. The velocities are evaluated under the standard conditions, and

another simulation is executed with a different configuration and permitted to run for longer total time. The results are grouped in Figure 3.23 and reveal a smoother representation of steady state realization.

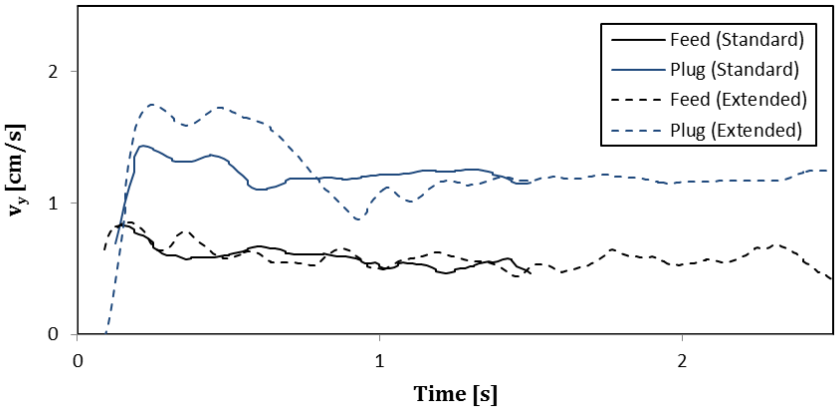

Figure 3.23 Velocity of feed and plug material over time for two configurations under standard conditions

This plot resembles a more classical time independence diagram at which transient zones converge to the same stable value. The study of the input (feed) and output (plug) velocities may be the best verification of the achievement of some steady state even when variation still exists in the internal system parameters. Once constant values are reached for external boundary motions, other natural oscillatory parameters, such as average roll pressure, can be time averaged over the stable domain.

CHAPTER 4: CONCLUSIONS AND FUTURE WORK

4.1 Conclusions

4.1.1 Summary

The application of MPFEM to the roll compaction process is presented in order to advance the understanding of the mechanics and micromechanics of the system, address the challenges of the methodology, and express the powerful and unique capabilities of the modeling technique.

Substantial attention is placed upon identifying the primary difficulties that limit practical implementation. This effort emphasizes mass scaling, ALE adaptive meshing, and contact optimization as the major tools assisting a successful MPFEM roll compaction model. In the end, relatively large particle systems are capable of being simulated in an admissible time frame and allow a sufficient description of the mechanics.

With an effective model, the many governing operating parameters are varied and analyzed to understand their impact on the overall process. Convergence in terms of mass density is an important step in validating the model while convergence in gap ratio opens questions to the importance of the wall effect and stress chain stability preservation. Parametric studies are undergone for feed stress, roll speed, and friction. Moderate changes in roll speed are expected and determined to not prominently increase or decrease the output of the system. This result is an outcome of the quasi-static nature of the

problem. On the other hand, increasing feed pressure and coefficients of friction is shown to build compaction pressure between the rolls. In the case of friction, the chosen conditions determine the occurrence of overcompaction and jamming (large friction) or undercompaction and particle flow (low friction). These extremes isolate a region in a frictional space that corresponds to adequate conditions for compaction. An analogous situation arises for feed pressure in which roll compactor failures such as overcompaction or undercompaction can develop if the pressure magnitude lies outside an acceptable range.

Further analysis depicts local mechanical responses of the system. Shear bands are observed through analyzing velocity, deviation, and gradient fields. These bands create asymmetrical motions across the roll gap and ultimately cause inconsistent variation inside the system. The irregular nature of the shear bands is a major candidate for the infrequent oscillations in the roll reaction forces and moments and may cause similar problems in experimental work. In addition, the effects of particle shape are investigated by comparing ellipse and hexagon simulations to the standard circle model. The role of morphology is found to control numerous aspects of the roll compaction mechanics. The hexagons interlocked and jammed the roll compactor while the ellipses drastically rotated in the slip zone and created a decreased density region between the entry and nip zone. Each of the particle shapes demonstrated unique behavior that can only be captured through a morphological analysis.

The local micromechanical investigations are instances of advantages achieved by performing an MPFEM simulation. For example, prediction of bulk density decreases due to local orientation variation cannot currently be explored by other modeling techniques. In addition, plasticity laws and discrete contact laws handling large deformation are not required. MPFEM controls many mechanical processes naturally and is, therefore, able to avoid assumptions and restricting conditions.

4.2 Future Work

4.2.1 Future Work

Roll compaction is a complex process influenced by a large variety and number of operating conditions. The application of MPFEM to this process is a modern approach with no prior historical precedence. Therefore, the presentation in this work can only offer a foundation and necessitates a full comprehensive study to explore the complete potential of the technique and to investigate all aspects of the problem. This analysis can only be achieved over time and with the diligence of numerous researchers. Recommendations are given in the following sections to suggest desirable areas of advancement. The future work is divided into two primary sections, i.e., modeling techniques and model extensions.

4.2.2 Improvements in Modeling Techniques

As emphasized in earlier discussions, the key factor hindering MPFEM's predictive capacity is the computational intensiveness. A number of methods

were proposed to reduce the amount of required computational resources. However, there are many enhancements that could significantly decrease simulation time and promote solution accuracy.

An improved contact detection system could be developed to adaptively respond to missed contacts. This system would minimize the contact range defined a priori, and it would determine if a contact was missed after a certain number of time steps. If a contact was lost, the simulation would recognize it, define the new contact pair, and restart the analysis at the previous mark. This adaptive technique would minimize the number of contact pairs needed to be checked during the analysis. Another possible method for simulation time reduction would involve the elimination of elements. Wasted calculations are performed on particles rearranging above the roll entry and flowing after the roll exit. The exiting particles should instead be transferred back to the top of the feed zone. A suggestion for accomplishing this task would involve using more than one feed bar at the top of the feed. Instead, particles could be placed into bins, and as the lower bar approaches the roll, it is removed and reinstated at the top of the feed with new particles underneath. This strategy would require thin bars to deliver the feed pressure to the rolls in order to minimize oscillations. Adaptive mass scaling approaches may also greatly benefit the practicality of MPFEM. Employing mass scaling is the major reason why one of these simulations is able to be implemented in a reasonable time frame. If the mass scaling was focused and optimized to regions needing the scaling while leaving

other elements unchanged, the solution will become more accurate and not require as much time. For example, smaller elements naturally possess smaller characteristic lengths. These lengths restrict the stable time step more than their larger counterparts and should therefore be mass scaled accordingly.

Meshing techniques can also be improved to assist solution accuracy. As particles progress through the rolls, the compaction pressure forces their shapes into become increasingly anisotropic. The mesh needs to adapt to this scenario. A mesh solution for a deformed particle between the rolls could be mapped to the same particle with a new "clean" anisotropic mesh. This process would relieve highly deformed elements while preparing the particle for further deformation in an oriented manner. Furthermore, ALE adaptive meshing should be scrutinized and optimized to reduce computation time and memory usage.

4.2.3 Model Extensions

The MPFEM roll compaction model can be extended in many ways to include new features or to more thoroughly address a particular aspect. There are numerous parametric studies that can be performed to understand other specific mechanical responses.

Some parametric studies for future simulations should consider dimensionless roll gap, particle size distributions, initial configuration (order and disorder in arrangement), and ratio of elastic modulus to yield strength. Each of the studies presented in this work could also be deeply investigated. Larger

ranges of frictional coefficients and particle shapes can be explored to represent a full depiction of each behavior.

Extensions could also be appended to the current model to observe a more realistic system. For example, a floating roll is typically implemented in industry where one roll is unconstrained in the x direction, allowing the roll gap to adapt and continuously supply a constant pressure. Rolls have indentations tooled into their surfaces to improve grip. This geometric effect can be modeled in MPFEM by varying the connectivity of the rigid roll surface. MPFEM could be used to analyze mixtures of particles with various properties or sizes, which is another geometric and definition modification to the system. The constitutive model of the particle behavior itself could be modified; particles are porous materials that could be modeled with a more accurate plasticity law. Lastly, the feed boundary condition could be adjusted to match a more appropriate depiction of the screw feed, such as a periodic pressure along the feed surface.

A major model extension that requires a revisit is the execution of a cohesion law for MPFEM roll compaction. Cohesion is an important factor in the roll compaction process that influences the mechanical behavior down to the particulate scale. However, implementation in Abaqus for two dimensional discrete simulations is not easily achieved and could not be successfully performed. An attempt was also carried out in three dimensional space where thin cylinders acted as the circular particles. This effort was unsuccessful due to several numerical issues concerning the damage evolution and cohesion laws,

and so full cohesion was tried. Full cohesion is executed through the no separation condition imposed on contact pairs in 2D. Although the full cohesive model simulated for some amount of time, numerical problems developed very quickly and ended the analysis. Thus, the exploration into a working cohesion model is a topic for future work and a very important subject for roll compaction. If using Abaqus, a recommendation would be to implement cohesion through a user defined subroutine.

Some results of the roll compaction process were achieved in a preliminary fashion and not presented in the current work. These investigations included illustrating the determination of the nip angle (velocity profile tangential to the roll), pressure and shear stress distribution along the roll, equivalent plastic strain analysis, and the calculation of coordination number and contact area for each particle. In addition, a direct comparison between roll compaction and die compaction in MPFEM is of great interest. These topics are all subjects of future work and can provide excellent insight into the roll compaction process.

LIST OF REFERENCES

1. Parikh, D.M., *Handbook of Pharmaceutical Granulation Technology*. Vol. 81. 1997: CRC Press.

2. Cunningham, J.C., D. Winstead, and A. Zavaliangos, *Understanding Variation in Roller Compaction Through Finite Element-Based Process Modeling.* Computers & Chemical Engineering, 2010. **34**(7): p. 1058-1071.

3. Kleinebudde, P., *Roll Compaction/Dry Granulation: Pharmaceutical Applications.* Eur J Pharm Biopharm, 2004. **58**(2): p. 317-26.

4. Johanson, J.R., *A Rolling Theory for Granular Solids.* Journal of Applied Mechanics, 1965. **32**(4): p. 842-848.

5. Jenike, A. and R. Shield, *On the Plastic Flow of Coulomb Solids Beyond Original Failure.* J. appl. Mech, 1959. **26**(4): p. 599-602.

6. Bindhumadhavan, G., et al., *Roll Compaction of a Pharmaceutical Excipient: Experimental Validation of Rolling Theory for Granular Solids.* Chemical Engineering Science, 2005. **60**(14): p. 3891-3897.

7. Katashinskii, V.P., *Analytical Determination of Specific Pressure During the Rolling of Metal Powders.* Powder Metallurgy and Metal Ceramics, 1965. **5**(10): p. 765-772.

8. Dec, R.T., A. Zavaliangos, and J.C. Cunningham, *Comparison of Various Modeling Methods for Analysis of Powder Compaction in Roller Press.* Powder Technology, 2003. **130**(1-3): p. 265-271.

9. Cunningham, J.C., *Experimental Studies and Modeling of the Roller Compaction of Pharmaceutical Powders*, 2005, Drexel University: Philadelphia, PA. p. 1-247.

10. Drucker, D.C., R.E. Gibson, and D.J. Henkel, *Soil Mechanics and Work Hardening Theories of Plasticity.* Transactions of the American Society of Civil Engineers, 1957. **122**: p. 338-346.

11. DiMaggio, F.L. and I.S. Sandler, *Material model for granular soils.* Journal of the Engineering mechanics Division, 1971. **97**(3): p. 935-950.

12. Sandler, I.S., G.Y. Baladi, and F.L. DiMaggio, *Generalized cap model for geological materials.* Journal of the Geotechnical Engineering Division, 1976. **102**(7): p. 683-699.

13. Brown, S. and G. Abou-Chedid, *Yield behavior of metal powder assemblages.* Journal of the Mechanics and Physics of Solids, 1994. **42**(3): p. 383-399.

14. Han, L.H., et al., *A Modified Drucker-Prager Cap Model for Die Compaction Simulation of Pharmaceutical Powders.* International Journal of Solids and Structures, 2008. **45**(10): p. 3088-3106.

15. Cunningham, J., I. Sinka, and A. Zavaliangos, *Analysis of tablet compaction. I. Characterization of mechanical behavior of powder and powder/tooling friction.* Journal of pharmaceutical sciences, 2004. **93**(8): p. 2022-2039.

16. Sinka, I., J. Cunningham, and A. Zavaliangos, *Analysis of tablet compaction. II. Finite element analysis of density distributions in convex tablets.* Journal of pharmaceutical sciences, 2004. **93**(8): p. 2040-2053.

17. Procopio, A.T., A. Zavaliangos, and J.C. Cunningham, *Analysis of the Diametrical Compression Test and the Applicability to Plastically Deforming Materials.* Journal of Materials Science, 2003. **38**(17): p. 3629-3639.

18. Balicki, M., *Numerical Methods for Predicting Roll Press Powder Compaction Parameters*, 2003, Ecole Des Mines D'Albi-Carmaux.

19. Muliadi, A.R., J.D. Litster, and C.R. Wassgren, *Modeling the Powder Roll Compaction Process: Comparison of 2-D Finite Element Method and the Rolling Theory for Granular Solids (Johanson's Model).* Powder Technology, 2012. **221**(0): p. 90-100.

20. Dec, R. and R. Komarek. *Testing Performance of Roll Press Force Feed Systems*. in *BIENNIAL CONFERENCE-INSTITUTE OF BRIQUETTING AND AGGLOMERATION*. 1993. INSTITUTE OF BRIQUETTING AND AGGLOMERATION.

21. Cundall, P.A. and O.D. Stack, *A Discrete Numerical Model for Granular Assemblies.* Geotechnique, 1979. **29**(1): p. 47-65.

22. Harthong, B., D. Imbault, and P. Dorémus, *The Study of Relations Between Loading History and Yield Surfaces in Powder Materials Using Discrete Finite Element Simulations.* Journal of the Mechanics and Physics of Solids, 2012. **60**(4): p. 784-801.

23. Harthong, B., et al., *Modeling of High-Density Compaction of Granular Materials by the Discrete Element Method.* International Journal of Solids and Structures, 2009. **46**(18–19): p. 3357-3364.

24. Benson, D.J., *An Analysis by Direct Numerical Simulation of the Effects of Particle Morphology on the Shock Compaction of Copper Powder.* Modelling and Simulation in Materials Science and Engineering, 1994. **2**(535).

25. Meyers, M.A., D.J. Benson, and E.A. Olevsky, *Shock Consolidation: Microstructurally-Based Analysis and Computational Modeling.* Acta Materialia, 1999. **47**(7): p. 2089-2108.

26. Gethin, D.T., et al., *Numerical Comparison of a Deformable Discrete Element Model and an Equivalent Continuum Analysis for the Compaction of Ductile Porous Material.* Computers & Structures, 2001. **79**(13): p. 1287-1294.

27. Gethin, D.T., R.W. Lewis, and R.S. Ransing, *A Discrete Deformable Element Approach for the Compaction of Powder Systems.* Modelling and Simulation in Materials Science and Engineering, 2003. **11**(1).

28. Kou, S.Q., et al., *Numerical Investigation of Particle Breakage as Applied to Mechanical Crushing—Part II: Interparticle Breakage.* International Journal of Rock Mechanics and Mining Sciences, 2001. **38**(8): p. 1163-1172.

29. Procopio, A.T. and A. Zavaliangos, *Simulation of Multi-Axial Compaction of Granular Media from Loose to High Relative Densities.* Journal of the Mechanics and Physics of Solids, 2005. **53**(7): p. 1523-1551.

30. Procopio, A.T., *On the Compaction of Granular Media Using a Multi-Particle Finite Element Model*, 2007, Drexel University: Philadelphia, PA. p. 1-151.

31. Zavaliangos, A. *A Multiparticle Simulation of Powder Compaction Using Finite Element Discretization of Individual Particles*. in *MRS Proceedings*. 2002.

32. Laarhoven, P.M. and E.L. Aarts, *Simulated Annealing*, in *Simulated Annealing: Theory and Applications*. 1987, Springer Netherlands. p. 7-15.

33. El-Sakhawy, M. and M.L. Hassan, *Physical and Mechanical Properties of Microcrystalline Cellulose Prepared from Agricultural Residues.* Carbohydrate Polymers, 2007. **67**(1): p. 1-10.

34. *Abaqus 6.8-2 Analysis Users Manual*, 2008, Dassault Systèmes Simulia Corp.: Providence, RI.

35. Fazekas, S., et al., *Morphologies of three-dimensional shear bands in granular media.* Physical Review E, 2006. **74**(3): p. 031303.

36. Cho, G., J. Dodds, and J. Santamarina, *Particle Shape Effects on Packing Density, Stiffness, and Strength: Natural and Crushed Sands.* Journal of Geotechnical and Geoenvironmental Engineering, 2006. **132**(5): p. 591-602.

37. Odagi, K., T. Toshitsugu, and Y. Tsuji, *Compressive Flow Propety of Powder in Roll-type Presses - Numerical Simulation by Discrete Element Method.* Journal of the Society of Powder Technology, 2001(38): p. 150-159.